Dynamic regulation of protein homeostasis underlies acquired thermotolerance in Arabidopsis

Mayur Bajaj[1], Annapurna Devi Allu[1*], Basuthkar J Rao[1,2*]

[1]Department of Biology, Indian Institute of Science Education and Research (IISER), Tirupati - 517619, INDIA

[2]Department of Animal Biology, School of Life Sciences, University of Hyderabad, Hyderabad - 500046, INDIA

* Co-corresponding authors – anu.allu@iisertirupati.ac.in; bjrao@uohyd.ac.in

Abstract

Rapid climate change demands the development of heat-resilient plants. Elevated temperatures perturb cellular protein homeostasis, and its timely restoration is crucial for plant survival after stress. Thermopriming, which involves pre-exposure to sublethal heat stress, has emerged as a promising strategy for enhancing heat stress tolerance. However, the impact of thermopriming on protein homeostasis remains unclear. Here, we demonstrate that priming-mediated acquired thermotolerance involves the dynamic regulation of protein maintenance and clearance mechanisms. Priming facilitates the activation of heat shock response (HSR) via HSFA1, and unfolded protein response (UPR). Simultaneously, priming induces the protein clearance pathway, namely autophagy, potentially through the dynamic modulation of autophagy-negative regulators. Contrastingly, unprimed seedlings fail to mount HSR and UPR, resulting in disrupted proteostasis and the accumulation of aggregates, and ultimately fail to survive. While the loss of UPR was found to have a minimal impact on priming-mediated outcomes, the HSR response proved essential, as its absence led to lethality under heat stress. Additionally, the absence of HSR was found to enhance the autophagy response post-stress. Our results highlight the critical role of protein maintenance mechanisms over clearance pathways in ensuring survival. Taken together, our study demonstrates that thermopriming enhances heat stress resilience by temporally coordinating autophagy, HSR and UPR responses to maintain proteostasis.

Keywords

Autophagy, Heat Shock Factor A1, Priming, Proteostasis, Unfolded Protein Response, Thermotolerance

Introduction

In nature, plants often encounter multiple abiotic and biotic stressors that affect their cellular homeostasis. High temperatures are one such abiotic stressor that is detrimental to plant growth, productivity and even survival. Heat stress reduces protein, starch, and oil content (Fahad et al., 2017) and can lead to substantial economic losses in agriculture (Long & Ort, 2010; Schmitt et al., 2022). Studies have reported that for every 2°C rise in temperature, there could be a 50% decline in crop productivity (Lobell et al., 2012). As sessile organisms, plants cannot escape adverse conditions and must instead preemptively activate protective genes to survive. Recent studies have shown that pre-exposure to a stress stimulus (referred to as 'priming') can dramatically improve plant stress tolerance (Liu et al., 2022; Samantaray et al., 2023).

'Priming' refers to the pre-conditioning with non-lethal stress treatment used to induce acquired stress tolerance. The priming treatment allows the plant to robustly respond to a subsequent severe stress, referred to as 'triggering' (Bäurle, 2016; Conrath et al., 2007; Sedaghatmehr et al., 2016; Wilkinson et al., 2019). Several stimuli, including mild environmental stress factors, hormones or chemical moieties can serve as priming agents (Nair et al., 2022). Priming-mediated acquired stress tolerance has been previously studied in the model plant system *Arabidopsis thaliana* (hereafter referred to as Arabidopsis) along with several crop plants (Balmer et al., 2018; Liu et al., 2022; Samantaray et al., 2023; Song et al., 2015; Ye et al., 2019). Priming can aid in remodeling the transcriptomic, epigenetic, or metabolic programs, thereby increasing the robustness of plant responses to subsequent stress (Catoni et al., 2022; Espinas et al., 2016; Gamir et al., 2014; Serrano et al., 2019; Tugizimana et al., 2018). Although several studies have focused on understanding the transcriptional and epigenetic regulation underlying the priming response (Crespo-Salvador et al., 2018; Kotkar & Giri, 2020; Nair et al., 2022; Noh et al., 2021), very little is known about the role of post-translational processes such as protein homeostasis, autophagy and mitochondrial dynamics, which are critical for plant survival (Raffeiner et al., 2023; Selinski et al., 2024; Sun et al., 2021).

Heat stress primarily disrupts protein homeostasis by destabilizing thermolabile proteins (Richter et al., 2010). In response, plants activate multiple proteostasis pathways - including molecular chaperones, autophagy, and the ubiquitin-proteasome system (UPS) - to restore protein homeostasis and promote stress tolerance. Upon heat stress, misfolded proteins accumulate thereby activating heat shock response (HSR) and unfolded protein response (UPR) (Gao et al., 2023). HSR involves accumulation of heat

88 shock proteins (HSPs), which facilitates the refolding and disaggregation of misfolded proteins (Richter
89 et al., 2010; Rosenzweig et al., 2019). *HSFA2* and *HSFA3* are well-established HSR molecules involved
90 in transcriptional upregulation of chaperones under acclimatizing heat stress conditions (Friedrich et al.,
91 2021). The UPR in plants is a complex endoplasmic reticulum (ER)-associated pathway which involves
92 activation of multiple transducers, including members of the IRE1, bZIP and NAC families to resolve
93 proteotoxic stress (Nawkar et al., 2018; Pastor-Cantizano et al., 2020). Additionally, proteotoxic stress
94 also activates degradative pathways such as UPS and autophagy. Where UPS is involved in clearance
95 of unfolded/misfolded proteins, autophagy contributes by removing damaged organelles and promotes
96 the recycling of dysfunctional proteins/aggregates during heat stress (Raffeiner et al., 2023; Sharma et
97 al., 2024; Su et al., 2020; Zhou et al., 2013). Autophagy is tightly regulated by signaling pathways
98 involving TOR, SnRK, and IRE1. TOR (target of rapamycin) inhibits autophagy under nutrient-rich
99 conditions by phosphorylating components of the autophagy initiation complex (Suttangkakul et al.,
100 2011), whereas, SnRK (sucrose non-fermenting 1 (SNF1)-related protein kinase) promotes autophagy
101 during energy deprivation by inhibiting TOR (Soto-Burgos & Bassham, 2017). IRE1 (Inositol-requiring
102 1), an ER-membrane protein, is proposed to positively regulate autophagy via its mRNA degradation
103 activity (Bao et al., 2018). Additionally, HSFA1a has also been identified to induce autophagy under
104 heat and drought stress by upregulating *ATG* genes (Wang et al., 2015; Xie et al., 2022). Autophagy
105 also plays a role in resetting long-term heat-stress memory (Sedaghatmehr et al., 2019) by degrading
106 specific chaperones HSP21 and HSP90.1, through FtsH6- and NBR1-mediated mechanisms,
107 respectively (Sedaghatmehr et al., 2021; Thirumalaikumar et al., 2020). However, holistically, how
108 protein homeostasis mechanisms contribute towards priming-mediated responses remain unclear.

109 In this study, we examined the dynamics and regulation of proteostasis pathways to gain insights into
110 the post-translational landscape during priming-mediated acquired thermotolerance. Our findings
111 suggest that short-term thermopriming enhances tolerance to severe heat stress by concurrently
112 activating protein protective responses through the accumulation of chaperones and folding catalysts
113 via HSR and UPR; and facilitates clearance of damaged proteins via dynamic modulation of autophagy.
114 Conversely, when exposed to heat stress, unprimed seedlings fail to activate protein protective
115 responses, experience translational arrest, accumulate protein aggregates, leading to disruption of
116 proteostasis and ultimately fail to survive. Overall, our study offers novel insights into priming-mediated
117 thermotolerance and highlights the critical role of protein homeostasis in maintaining cellular resilience
118 under heat stress.

119 # Results

120 ## Priming improves survival from severe heat stress

121 To understand the mechanisms driving short-term acquired thermotolerance, we exposed the five-day-
122 old Arabidopsis wild-type (WT) seedlings to 37°C (for 90 min) and allowed them to briefly recover at
123 optimum conditions (for 90 min) before exposing them to triggering heat stress (45°C for 45 min)
124 (**Figure 1A**). Hereafter, this condition is referred to as 'primed'. The effect of thermopriming was
125 analysed by comparing the impact of lethal heat stress on primed *vs.* naive (unprimed: directly exposed
126 to triggering heat stress) seedlings. Post heat stress, seedling growth was recorded as a function of time
127 under all the conditions tested (control, primed and unprimed) (**Figure 1B**). Post-exposure to triggering
128 heat stress, primed seedlings displayed a halt in growth; however, the growth resumed quickly, which
129 was found to be significantly higher than the unprimed, quantified as leaf number, root length and fresh
130 weight (**Figure 1, C-E**). By 5 days post stress (DPS), unprimed seedlings display a visibly complete
131 loss of chlorophyll and fail to survive (**Figure 1B**). In summary, heat stress affects growth in both
132 primed and unprimed conditions. However, primed seedlings can mount a more robust response,
133 facilitating the swift resumption of growth after heat stress.

134 ## Thermopriming mitigates heat stress-induced protein damage

135 To determine the impact of heat stress (with or without priming) on protein homeostasis, we analysed
136 the protein content in seedlings across all conditions (**Figure 2A**). The total protein content in the control
137 (grown under optimal conditions at 22°C) and primed seedlings was found to be similar across all the
138 time points analysed post-heat stress (**Figure S1A**). In contrast, unprimed seedlings displayed a
139 consistent decline in total protein levels from 1 to 3 DPS, signifying a reduction in total protein content
140 (**Figure S1A**).

141 Heat stress causes protein denaturation, leading to the accumulation of misfolded/unfolded proteins,
142 which, if not resolved, can lead to severe consequences. Misfolded protein accumulation triggers the
143 splicing of *bZIP60u* (unspliced), forming *bZIP60* spliced form (*bZIP60s*), which is known to
144 transcriptionally modulate genes involved in restoring cellular proteostasis under stress conditions
145 (Deng et al., 2011; Humbert et al., 2012). To assess whether proteotoxic stress was induced in our
146 experimental regime, we analysed the transcript abundance of *bZIP60s* across all the conditions at
147 different time points post-priming/triggering stress (**Figure 2A**). Interestingly, exposure to priming

148 temperature itself triggered misfolded protein accumulation, as evidenced by the presence of *bZIP60s*
149 at AP time point (**Figure 2B; S1, B-C**). Following the triggering heat stress, while both primed and
150 unprimed seedlings accumulated misfolded proteins (elevated *bZIP60s* at AT/0 DPS), only primed
151 seedlings recovered to control levels by 1 DPS (**Figure 2B; S1, B-C**). The unprimed seedlings displayed
152 sustained proteotoxic stress as evidenced by elevated *bZIP60s* levels throughout the recovery phase
153 (**Figure 2B; S1, B-C**). These results suggest that priming-mediated responses may be involved in the
154 efficient maintenance of the protein pool. This prompted us to assess the status of protein homeostasis
155 maintenance pathways (i) heat shock response (HSR), (ii) unfolded protein response (UPR), and (iii)
156 autophagy response during our heat stress paradigm.

157 **Thermopriming facilitates effective heat shock response mediated by HSFA1**

158 We determined the HSR status (**Figure 2C**), by analysing chaperone levels (HSP70 and HSP90) post-
159 heat stress across all conditions. Exposure to the priming stimulus (AP) resulted in increased
160 accumulation of HSP70 and HSP90, which persists until 1 DPS post-exposure to triggering heat stress
161 in the primed, compared to the control (**Figure 2, D-E**). However, the unprimed seedlings failed to
162 mount such a response, with the levels of HSPs being lower than those of the control seedlings (**Figure**
163 **2, D-E**). In addition, we analysed the abundance of other heat stress inducible proteins HSP17.6, HSP21
164 and HSP101 (Bäurle, 2016; Friedrich et al., 2021) at all the time points stated above. Increased levels
165 of all three HSPs were detected in the primed, but not in the unprimed or control seedlings (**Figure 2,**
166 **F-G**). Immediately upon exposure to priming (AP), an increased abundance of HSP17.6, HSP21 and
167 HSP101 was detected (**Figure 2F**), which persisted until 3 DPS (**Figure 2G**). Furthermore, to assess
168 whether the HSP abundance observed thus far parallels transcript levels across all conditions, we
169 profiled the expression of *HSPs* using data available from RNA-sequencing (**Figure S2, A-C**), followed
170 by confirmation using qPCR. In the primed seedlings, the abundance of HSPs correlated with their
171 elevated transcript levels compared to those of the control (**Figure 2H; S2D**). Surprisingly, unprimed
172 seedlings displayed a gradual increase in *HSPs* transcript abundance post-heat stress (**Figure 2H; S2D**),
173 which did not correlate with the observed protein levels (**Figure 2, D-G**).

174 Furthermore, we examined the involvement of HSFA1, a core regulator of the plant heat stress response
175 (Bakery et al., 2024). We profiled the expression of *HSFA1a* and its direct and indirect downstream
176 targets, *HSFA2* and *HSFA3* (Ohama et al., 2017), following heat stress. We observed that *HSFA1a*
177 levels did not change significantly across the time points tested, except at the AT/1DPS in unprimed

178 (**Figure S2E**). These observations are in line with previous reports where *HSFA1a* levels did not change
179 significantly (Löchli et al., 2023), likely because HSFA1's regulation under heat stress is predominantly
180 controlled at the post-translational level (Mesihovic et al., 2022; Ohama et al., 2017; Wang et al., 2023).
181 In contrast, the downstream targets *HSFA2* and *HSFA3* were upregulated in both primed and unprimed
182 following heat stress (**Figure S2E**). Notably, *HSFA2* induction persisted even at 2 DPS, whereas *HSFA3*
183 induction returned to basal levels by 1 DPS in primed seedlings (**Figure S2E**).

184 HSFA1s are a well-established HSR regulator involved in transcriptional upregulation of chaperones
185 (Ohama et al., 2017). In our study, we observed HSFA1a's downstream activity (*HSFA2/HSFA3* levels)
186 to be correlated with the abundance of *HSPs* across our regime. These observations prompted us to
187 assess the impact of HSFA1s loss on the priming-mediated heat stress response. To overcome the
188 functional redundancy of the HSFA1s in Arabidopsis, we used a previously reported *hsfa1a/b/d* triple
189 mutant line (Yoshida et al., 2011) for our analysis. The unprimed *hsfa1a/b/d* and Col-0/Ws-0 did not
190 show any differences in their basal heat stress response (**Figure 2I**). However, even upon priming, the
191 *hsfa1a/b/d* mutants failed to survive following heat stress, unlike the Col-0/Ws-0 seedlings (**Figure 2I**).
192 Furthermore, priming-mediated HSP induction was abolished in the *hsfa1a/b/d* mutant in contrast to the
193 WT (**Figure 2J**). These findings underscore the essential role of HSFA1s in mediating priming-
194 dependent chaperone induction and thermotolerance.

195 **Unprimed seedlings experience translational arrest following heat stress**

196 Notably, despite the activation of HSFA1 and the concurrent increase in *HSP* transcript levels, unprimed
197 seedlings failed to show a corresponding increase in HSP protein abundance. This prompted us to check
198 the translational status across these conditions. To this end, we examined the expression profiles of
199 differentially expressed genes (DEGs) involved in protein translation using our transcriptome data. We
200 observed that exposure to priming stimulus alone (AP time point) has a minimal impact on the
201 expression levels of genes encoding RNA polymerases and ribosomal proteins. However, exposure to
202 triggering stimulus (AT timepoint) led to a severe downregulation of these genes, indicating a repression
203 of translation (**Figure S3A**). Interestingly, during the heat-stress recovery phase, the expression of these
204 genes was restored to near-control levels in the primed seedlings, whereas, the unprimed seedlings
205 exhibit a sustained downregulated gene expression, suggesting a sustained halt in translation (**Figure**
206 **S3A**). These findings corroborate our earlier observation that although *HSP* transcript accumulates in
207 the unprimed, the lack of HSP induction is likely due to impaired translation.

208 **Priming activates the transcriptional unfolded protein response**

209 Dysregulation of protein homeostasis is known to impact ER functional status, triggering the activation
210 of unfolded protein response (Humbert et al., 2012; Nawkar et al., 2018). The UPR aims to restore ER-
211 proteostasis by upregulating genes involved in ER-quality control (ERQC) and ER-associated
212 degradation (ERAD) pathways (Duan et al., 2023; Nawkar et al., 2018). To assess the status of UPR,
213 we examined the expression profiles of DEGs involved in ERQC and ERAD pathways. We observed
214 that priming stimulus alone can lead to an increase in the expression of several canonical UPR
215 components, including members of the bZIP and NAC transcription factor families, as well as luminal
216 binding proteins (BIPs), protein disulfide isomerases (PDILs), ER-resident DnaJ proteins (ERDJs
217 /P58IPK) and others, which are indicative of early ERQC activation (**Figure 3A**). Additionally, the
218 upregulation of various ubiquitin ligases implicated in the ERAD pathway was also observed upon
219 priming (**Figure 3A**). Importantly, this transcriptional upregulation persisted in primed seedlings even
220 at the post-triggering time point. In contrast, despite experiencing heat stress, unprimed seedlings failed
221 to exhibit any increase in the abundance of these transcripts (**Figure 3A**). These results indicate that
222 priming enables transcriptional activation of the UPR in response to heat stress.

223 To further evaluate whether the loss of UPR impacts priming-mediated responses, we subjected *bzip60*
224 and *ire1a ire1b* (referred to as *ire1a/b*) homozygous mutants to our experimental regime. The IRE1-
225 bZIP60 signalling axis is one of the major branches of plant UPR. Upon ER stress, IRE1 is activated,
226 leading to the formation of *bZIP60s*, which are known to transcriptionally modulate a subset of genes
227 involved in the ERQC/ERAD pathways of the UPR (Nawkar et al., 2018; Pastor-Cantizano et al., 2020).
228 The dynamics of *bZIP60s* accumulation during the experimental regime are shown in **Figure 2B**. When
229 directly exposed to triggering heat stress (unprimed), both *bzip60* and *ire1a/b* seedlings failed to survive,
230 similar to WT (Col-0) (**Figure 3B**). The primed UPR mutants were able to survive severe heat stress
231 upon priming (**Figure 3B**); however, their growth recovery post-stress was found to be slower compared
232 to WT. When observed at seven days post-stress, the root length was found to be significantly lower in
233 the primed *bzip60* and *ire1a/b* compared to their respective controls, while the root length of primed
234 WT was found to be similar to its control (**Figure 3C**). When comparing fresh weight, primed seedlings
235 of all genotypes exhibited lower fresh weights than their respective controls (**Figure 3D**).

236 As the UPR mutants can survive severe heat stress following priming treatment, we further evaluated
237 whether the loss of UPR influences the HSR. For this, we assessed the chaperone abundance in the

238 *bzip60* and *ire1a/b* mutants. Primed *bzip60* and *ire1a/b* seedlings displayed elevated levels of all the
239 HSPs tested (**Figure 3E**). However, slight differences still existed in the HSP abundance dynamics
240 across genotypes. For instance, HSP17.6 and HSP21 showed similar induction patterns across WT and
241 *ire1a/b*, wherein both the HSPs reached maximal induction by 1 DPS, whereas the *bzip60* mutant
242 displayed a maximum level of HSP21 at 2 DPS (**Figure S4A**). Nonetheless, primed WT showed a
243 slightly higher abundance of both HSP17.6 and HSP21 at 0 DPS compared to *bzip60* and *ire1a/b*.
244 Similarly, both mutants displayed differences in the induction of HSP70 and HSP101 compared to WT.
245 The induction of HSP101 was highest in WT compared to the mutants at 0 DPS post-heat stress, which
246 declined from 0 to 3 DPS. Both the mutants displayed the highest abundance only at 1 DPS, whereas
247 *bzip60* showed a steady decline from 1 to 3 DPS (**Figure S4A**). For HSP70, the level of induction in
248 the mutants and WT was minimal, compared to other HSPs, at all the time points tested (**Figure S4A**).
249 Unprimed *bzip60* and *ire1a/b* displayed no detectable levels of HSPs (**Figure 3E**), similar to the
250 unprimed WT. To assess if the protein level changes parallel the transcript level changes, we determined
251 the expression of *HSPs* in both mutants. As expected, all the *HSPs* tested displayed elevated transcript
252 levels in both primed *bzip60* and *ire1a/b* (**Figure S4B**). Unprimed *bzip60* and *ire1a/b* also displayed a
253 delayed increase in *HSP* transcript levels (**Figure S4B**), similar to WT (**Figure S2D**). Together, these
254 results suggest that, unlike HSR, the UPR signalling is not essential for seeding survival upon priming;
255 however, it may be required for efficient growth recovery post-heat stress.

256 **Primed seedlings exhibit temporally regulated autophagy**

257 After assessing the dynamics of protein maintenance pathways, we next examined the status of the
258 protein clearance mechanism in response to priming/triggering heat stress. Autophagy, as a clearance
259 pathway, is known to be regulated at both transcriptional and post-translational levels. Transcriptionally,
260 autophagy activation involves the upregulation of autophagy-related genes (ATGs) (Wang et al., 2020;
261 Zhou et al., 2014), whereas at the protein level, autophagy induction is marked by the lipidation of
262 ATG8 to ATG8-PE, a critical step for autophagosome formation (Huang et al., 2022). Upon exposure
263 to priming-stimulus, several *ATGs* were upregulated in the primed seedlings, which was not observed
264 post-triggering stress in both primed and unprimed conditions (**Figure 4A**).

265 We next quantified the protein level autophagy response by using ATG8 as a marker. We observed that
266 exposure to the priming temperature alone could induce ATG8 levels (**Figure 4B**), as also reflected
267 from transcriptome data. However, immediately after exposure to triggering heat stress (0h), autophagy

268 (ATG8-PE) levels peaked in both primed and unprimed seedlings compared to the control (**Figure 4B**).
269 To assess if the heat stress-induced autophagy sustains, declines or surges with time, we checked the
270 ATG8-PE levels from 1 to 3 DPS. In the unprimed seedlings, the ATG8-PE levels increased further by
271 1 DPS, which continued until 2 DPS (**Figure 4C**). Notably, the visible decline in ATG8 levels (at 3
272 DPS) correlated with the reduced protein content in the unprimed seedlings (**Figure S1A**). However, in
273 the primed seedlings, ATG8-PE levels declined by 1 DPS to levels comparable to the control (**Figure**
274 **4C**). We also measured the autophagy flux across our paradigm using the GFP-ATG8 processing assay
275 (Kang et al., 2018; Shin et al., 2014). Autophagy flux, as measured by the free-GFP to total-GFP ratio,
276 was high in unprimed seedlings, indicating highly active autophagy compared to primed and control
277 (**Figure 4D**). Such an increase *vs.* decrease in autophagy levels in the unprimed *vs.* primed, respectively,
278 suggests a dynamic regulation of autophagy across these conditions.

279 **Regulation of autophagy under heat stress is TOR and SnRK-independent**

280 Previous studies have identified the role of TOR and SnRK in the regulation of autophagy under stress
281 (Pu et al., 2017; Soto-Burgos & Bassham, 2017). We wondered if TOR/SnRK are involved in the
282 priming-mediated regulation of autophagy under heat stress. To test this, we analysed the phospho-S6K
283 (pS6K) levels as a measure of TOR kinase activity (Upadhyaya et al., 2020) and active-SnRK (pAMPK:
284 using phospho-AMPKα antibody) for SnRK activity (Baena-González et al., 2007; Belda-Palazón et
285 al., 2020). Interestingly, neither pS6K (**Figure S5, A-B**) nor the pAMPK levels (**Figure S5, C-D**) were
286 altered across all the conditions. These findings suggest that heat stress induced autophagy (as observed
287 in **Figure 4, B-C**) is independent of TOR and SnRK mediated regulation.

288 **Priming-mediated autophagy induction is associated with attenuation of autophagy inhibitors**

289 The UPR regulator IRE1 has also been linked to modulate autophagy by fine-tuning its RIDD
290 (Regulated IRE1-dependent decay of mRNA) activity (Li & Howell, 2021; Maurel et al., 2014).
291 Notably, RIDD leads to the downregulation of inhibitors of autophagy, such as *BGLU21*, *ROSY1* and
292 *PR-14,* by targeting those mRNAs for degradation (Bao et al., 2018). We surmised that reversal to basal
293 level *vs.* more sustained autophagy in the primed *vs.* unprimed, respectively, may involve RIDD-
294 mediated regulation. Therefore, we examined the steady state transcript levels of *BGLU21* and *PR-14*
295 across all the conditions. At the time points- post priming (AP), before triggering (BT) and after
296 triggering (AT: 0 DPS), primed seedlings showed a significant reduction in the transcript levels of both

297 the genes compared to the control (**Figure 4E**). However, by 1-2 DPS, we observed a recovery in their
298 transcript abundance (**Figure 4E**). In contrast, the transcript levels of *BGLU21* and *PR14* remained
299 significantly lower in unprimed seedlings at all the time points compared to the control (**Figure 4E**). In
300 particular, these changes in the transcript abundance correlated with the ATG8/ATG8-PE levels in these
301 seedlings. For instance, in the primed, reduced transcript abundance of these autophagy inhibitors
302 correlates with the induced autophagy (at AP, BT and AT). By 1-2 DPS, when the transcript abundance
303 of these inhibitors reverted to near control level, autophagy was found to return to basal level in the
304 primed (**Figure 4F**). Contrarily, sustained induction of autophagy aligns with reduced transcript
305 abundance of the autophagy inhibitors in the unprimed, post-exposure to triggering heat stress (**Figure**
306 **4F**). These observations suggest that priming modulates autophagy, potentially through the RIDD-
307 mediated attenuation of autophagy inhibitors.

308 Further, we assessed whether the autophagy dynamics are affected in the IRE1A/B, and its downstream
309 target, bZIP60, knockout mutants. Interestingly, we observed that autophagy remained induced in both
310 *bzip60* and *ire1a/b* mutants (**Figure S6, A-B**) and its dynamics were similar to those of WT (**Figure 4,**
311 **B-C**). Loss of IRE1A/B and bZIP60 did not seem to disrupt autophagy induction during heat stress.
312 This was surprising, as we observed that heat stress facilitated IRE1-dependent dynamic degradation of
313 autophagy inhibitors, thereby modulating autophagy. However, autophagy was still being induced in
314 *bzip60* and *ire1a/b* mutants. These findings suggest the involvement of additional IRE1-independent
315 mechanism that may operate during heat stress to regulate autophagy.

316 **Impairment of the protein protective response amplifies the protein clearance mechanisms**

317 Given the potential involvement of alternate mechanisms regulating autophagy, we next investigated
318 the role of HSFA1a, a transcription factor previously shown to induce autophagy under abiotic stress
319 conditions (Wang et al., 2015; Xie et al., 2022). Notably, we observed the induction of HSFA1 activity
320 and a parallel upregulation of *ATG* genes post-priming stimulus (**Figure 4A; S2E**). When we probed to
321 assess if autophagy response gets affected in the *hsfa1a/b/d* triple mutant, we observed that autophagy
322 remains active in both primed and unprimed as evidenced by the sustained accumulation of ATG8-PE
323 post-stress (**Figure 5A**), suggesting that the autophagy response may be under a broader multiple
324 regulatory system.

325 As we observed that the HSP induction was abolished in the *hsfa1a/b/d* mutant with or without priming

326 (**Figure 2J**), we accounted for all the protein level evidence and summarized it in a data-directed
327 illustration (**Figure 5B**). Collectively, as evidenced from primed WT, activation of protein protective
328 response (chaperone accumulation) facilitates a dynamic clearance response (autophagy) that subsides
329 during stress recovery (**Figure 5B**). However, as observed in unprimed (all genotypes) and primed
330 *hsfa1a/b/d* seedlings, failure to accumulate chaperones upon heat stress may facilitate the persistent
331 activation of autophagy, aimed to resolve stress, but ultimately leads to lethality (**Figure 5B**).

332 **Unprimed seedlings accumulate protein aggregates following triggering heat stress**

333 So far, our findings indicate that priming-mediated heat stress tolerance involves the accumulation of
334 chaperones and temporary activation of autophagy. To test whether these changes contribute to the
335 effective maintenance of protein homeostasis, we examined the proteostasis state by analysing protein
336 aggregates at 1 DPS, the time at which we observed differential autophagy between the primed and
337 unprimed conditions (**Figure 4C**). The unprimed seedlings displayed elevated ubiquitin-conjugated
338 aggregates compared to primed or control (**Figure 6A**). Additionally, size distribution analysis of the
339 aggregates using dynamic light scattering (DLS) clearly showed that the unprimed seedlings
340 accumulated a high proportion of larger aggregates (13.03nm, 460.1nm and 6662.6nm), whereas the
341 primed seedlings accumulated comparatively smaller aggregates (18.02nm, 174.1nm and 1977.0nm),
342 which were proportionally similar to control (24.9nm, 136.5nm and 1550.5nm) (**Figure 6B**). We also
343 compared the diffusion behavior of the aggregates by using the DLS data. BSA was used as a standard
344 monomeric protein control (8nm), and it exhibited the fastest (steepest) decay (**Figure 6C**). The
345 aggregates derived from the unprimed displayed the slowest decay, reflecting larger population sizes,
346 whereas the aggregates derived from the primed showed a comparatively faster decay, reflecting a
347 relatively smaller population (**Figure 6C**). The control samples showed a profile comparable to BSA.
348 Taken together, our study indicates that thermopriming facilitates timely activation of the heat shock
349 response, unfolded protein response and autophagy, thereby aiding in effective aggregate clearance, and
350 collectively promotes heat stress tolerance.

351 ## Discussion

352 In the current study, we demonstrated that the efficient regulation of protein homeostasis underlies
353 priming-mediated short-term acquired thermotolerance in Arabidopsis. Heat stress has a profound
354 impact on the thermolabile molecular complexes, resulting in protein dysfunction and aggregation

355 (McLoughlin et al., 2019; Mittler et al., 2012; Rosenzweig et al., 2019). Maintaining proteostasis under
356 stress requires a fine balance between timely refolding of proteins via robust chaperone activity, and the
357 efficient clearance of irreversibly damaged proteins through the action of disaggregases, autophagy,
358 and/or the UPS (Hartl et al., 2011; McLoughlin et al., 2019; Mogk et al., 2018). Disruption of this
359 balance can lead to proteotoxic stress, which ultimately compromises cellular viability. In this study,
360 we observed that direct exposure to heat stress severely affected the protein content in the unprimed
361 seedlings, which was alleviated in the primed seedlings. These observations are consistent with the
362 previous reports showing that protein content is reduced upon exposure to noxious heat stress (Gulen
363 & Eris, 2004; Nagy-Réder et al., 2022). We found that thermopriming facilitates an increase in
364 chaperone abundance and UPR activation along with a temporary autophagy response, which together
365 contribute to the maintenance of protein homeostasis.

366 The unprimed seedlings, even upon facing similar triggering heat stress, failed to accumulate HSPs
367 despite a significant expression at the transcript level. Such a failure to accumulate HSPs may stem from
368 HSP sequestration within aggregates or impaired translation post-stress. We observed that genes
369 involved in translation remained severely downregulated in unprimed seedlings compared to primed
370 post-heat stress. Additionally, HSP101, a critical disaggregase that coordinates with other HSPs to
371 resolve proteotoxic stress (McLoughlin et al., 2019), was also detected only in primed seedlings (**Figure**
372 **S3B**). Cumulatively, this suggests that the chaperone synthesis was completely impaired in the
373 unprimed seedlings. In addition, the unprimed seedlings displayed high levels of ubiquitinylated
374 insoluble proteins, a trend also reported in HSP101 deficient plants during heat stress (McLoughlin et
375 al., 2019). Similarly, Dannfald et al. (2025) showed that priming protects the global translational
376 potential under heat stress, whereas direct heat exposure leads to preferential decay of mRNAs.

377 Given the difference in autophagy response between primed and unprimed, we examined the role of
378 TOR/SnRK-dependent pathways, which are known to be involved in regulating autophagy (Signorelli
379 et al., 2019; Soto-Burgos & Bassham, 2017; Yang et al., 2023), However, we did not detect any changes
380 in TOR/SnRK activity under our experimental regime. Indeed, TOR-independent mechanisms have
381 been reported to modulate autophagy under oxidative and ER stress conditions (Pu et al., 2017). Since
382 we observed that thermopriming induced ER stress and subsequent UPR activation, we explored the
383 potential involvement of IRE1. IRE1-RIDD activity has been previously associated with autophagy
384 induction under tunicamycin treatment (ER-stress inducing agent), wherein RIDD-mediated

385 degradation of autophagy inhibitors was shown to promote autophagy (Bao et al., 2018). The findings
386 from the current study show that thermopriming facilitates a degradation of RIDD target transcripts,
387 which correlates with the induction of autophagy in primed seedlings. Similarly, in unprimed seedlings,
388 the prolonged autophagy induction was associated with sustained transcriptional downregulation of
389 autophagy inhibitors. While these observations suggest that RIDD activity influences autophagy by
390 modulating the abundance of autophagy inhibitors, the precise mechanism remains to be explored. Bao
391 et al. (2018) suggested that BGLU21 (β-glucosidase 21) and PR-14 (pathogenesis-related protein 14)
392 proteins might interfere with the lipidation of ATG8, a crucial step for autophagosome formation,
393 thereby affecting autophagy.

394 Notably, despite the loss of IRE1A/B or bZIP60, autophagy was still induced post-heat stress. Our
395 observations concur with the previous report that shows bZIP60 is dispensable for IRE1-dependent
396 autophagy induction during ER stress (Bao et al., 2018). Moreover, although autophagy was found to
397 be induced in *ire1b* mutants following 42°C heat treatment (Yang et al., 2016), autophagy was not
398 induced in *ire1b* and *ire1a/b* mutants under ER stress upon DTT or tunicamycin treatment (Bao et al.,
399 2018; Liu et al., 2012). Given that autophagy was still activated in *ire1a/b* following thermal priming,
400 we posit that alternative pathways may mediate heat-induced autophagy. When probed for the
401 involvement of a heat inducible transcriptional activator of autophagy, *viz.* HSFA1 (Löchli et al., 2023;
402 Wang et al., 2015; Xie et al., 2022), autophagy was found to be induced even in the *hsfa1a/b/d* mutant.
403 These observations suggest that the autophagy response involves a multilayered regulation, a feature
404 advantageous for sessile organisms to tackle challenging environments.

405 Previous studies have also implicated the involvement of NBR1 (next-to-BRCA1) and ATG8-
406 interacting protein 1 (ATI1), 2 (ATI2) and 3 (ATI3) in mediating selective autophagy (Jung et al., 2020;
407 Sjøgaard et al., 2019; Thirumalaikumar et al., 2020; Zhou et al., 2018). The autophagy response can
408 either be selective, which involves recognition by specific receptors followed by subsequent clearance
409 of damaged organelles/aggregates; or bulk, which facilitates the clearance of cytoplasmic debris in a
410 non-selective manner (Marshall & Vierstra, 2018). From our transcriptome data, we observed that
411 selective autophagy receptors such as NBR1 and ATI1/2/3A were upregulated in the primed seedlings
412 alone (**Figure S7**), suggesting that the observed autophagy response in these seedlings may potentially
413 be selective in nature. Contrastingly, bulk autophagy may operate in the unprimed, as we did not observe
414 any change in the expression of these receptors. Moreover, vacuolar cell death has been previously

415 correlated with high autophagic flux (Minina et al., 2013), a feature we observed in unprimed seedlings.
416 Given the present evidence, it is tempting to speculate that bulk autophagy drives the unprimed
417 seedlings towards vacuolar cell death, however, this requires further validation.

418 Additionally, analysis of the *bzip60* and *ire1a/b* knockout mutants under primed conditions revealed
419 reduced growth recovery post-stress compared to WT. Previous studies have reported that *bzip60* and
420 *ire1a/b* mutants exhibit severe growth retardation under chemically-induced ER stress conditions (Deng
421 et al., 2013; Pu et al., 2019). Primed *bzip60* and *ire1a/b* seedlings displayed an increase in HSP levels;
422 however, their response was delayed compared to WT. One possible explanation is attenuated/delayed
423 protein translation, a feature previously reported in *ire1a/b* mutants under ER stress (Yoo et al., 2024).
424 Notably, Yoo et al. (2024) also demonstrated that supplementation with synthetic chaperones mitigated
425 the effects of attenuated translation and growth retardation in *ire1a/b* mutants. Given that the *ire1a/b*
426 mutants accumulate chaperones during the tested regime, the priming stimulus facilitates a faster and
427 more robust recovery of these seedlings under stress. Taking together the observed altered dynamics of
428 HSP induction in UPR mutants, we suggest a potential crosstalk between the HSR and UPR pathways
429 during thermotolerance. We also observed that the *hsfa1a/b/d* mutant failed to survive heat stress even
430 upon exposure to a priming stimulus. Such a failure could arise due to the inability of the *hsfa1a/b/d*
431 mutant to induce HSPs, implying that efficient protein maintenance (by chaperones) is a critical
432 determinant of stress response outcomes. An earlier report suggested that autophagy contributes to the
433 degradation of HSP, as autophagy mutants showed prolonged chaperone accumulation (Sedaghatmehr
434 et al., 2019). However, our findings suggests that autophagy and chaperone response may act
435 cooperatively to modulate protein homeostasis, with the impairment of one pathway potentially
436 amplifying the activity of the other, as seen in *hsfa1a/b/d* where failure to induce HSPs is accompanied
437 by sustained autophagy. These evidences underscores the importance of maintaining a delicate balance
438 between protein -folding and -clearance machineries in restoring cellular homeostasis following stress.
439 The unprimed seedlings experience a collapse of this balance, as evidenced by the failure to accumulate
440 HSPs, lack of UPR activation, excessive aggregate buildup, and sustained autophagy, which ultimately
441 compromises their growth and survival (**Figure 7**).

442 Taken together, our study highlights that thermopriming facilitates the efficient maintenance of protein
443 homeostasis through the timely activation of HSR, UPR and autophagy, thereby aiding in seedling
444 survival upon experiencing severe heat stress. Furthermore, we identified that UPR activation is

important for timely seedling recovery post-stress, but it may not be essential for mounting thermotolerance. However, HSFA1-mediated HSR is indispensable for mounting a heat stress tolerance response. As we observe chaperone accumulation is affected in UPR mutants, further studies are required to understand the probable crosstalk between UPR and HSR pathways during thermotolerance. Additionally, how heat stress may facilitate the mounting of bulk vs. selective autophagy during acquired thermotolerance needs to be further understood. Collectively, our findings revealed that precise and coordinated regulation of protein folding and clearance pathways is a key determinant of thermotolerance in Arabidopsis.

Methods

Plant materials and growth conditions

Arabidopsis (Col-0-referred to as WT and Ws-0-referred to as Ws-0) seeds were surface sterilized by washing with 80% ethanol for 30 seconds (s) followed by 1% bleach for 3 minutes (min), and 3x washes with sterile double distilled water. Seeds were then sown on ½ Murashige and Skoog media with 1% sucrose and 0.8% agar powder. The seeds were stratified at 4°C for two days before being transferred to growth chambers with 16-hour (h) light and 8 h dark, 65% humidity. The five-day-old Arabidopsis seedlings were primed by exposing them to 37°C for 90 min, followed by a recovery at 22°C for 90 min, and heat-triggering at 45°C for 45 min. The unprimed seedlings were directly exposed to 45°C for 45 min. Control seedlings were maintained under optimal growth conditions (22°C, 16h light and 8h dark, 65% humidity) throughout the experiment. Seedlings were harvested at different stress recovery time points for gene expression and protein analysis. The treatment conditions described above were also used for the analysis of GFP-ATG8a (CS39996) and *bzip60* (CS813074) (both lines were obtained from ABRC (Arabidopsis Biological Resource Center)). The *ire1a/b* line was kindly obtained from Chen et al., (2013) and Pu et al., (2019). Homozygous *hsfa1a/b/d* (psi00284) line was obtained from RIKEN-BRC.

Physiological measurements

To determine the effects of priming or triggering heat stress on growth, the seedlings were analysed for leaf number, root length and fresh weight. Data on leaf number (48 seedlings from three independent experiments), primary root length (18 seedlings from three independent experiments) and fresh weight (three biological replicates) were collected and analysed. For Figure 1E, 16 seedlings were pooled to

474 form a single replicate, and for Figure 3D, individual seedling fresh weight was measured. For leaf
475 number measurements, both true leaves and cotyledons were considered. Root length was measured
476 using the ImageJ software (https://imagej.net/software/fiji/) (Schneider et al., 2012).

477 **RNA extraction and gene expression analysis**

478 For extracting RNA, approximately 40-50 mg of Arabidopsis seedlings were collected at several time
479 points (post-priming and triggering, and during recovery) and frozen in liquid nitrogen. The samples
480 were ground using Retsch Miller MM400 at 25Hz for 30 s (x2 cycles). After grinding, RNA was isolated
481 from the samples using a combination of TRIzol/chloroform extraction and kit method (PureLink™
482 RNA Mini Kit, Thermo; 12183018A). The purified RNA was treated with DNase I (NEB; M0303)
483 following standard protocol. cDNA was synthesized using 1 µg of RNA following the manufacturer's
484 instructions (1st strand cDNA synthesis kit, Takara; 6110A). For gene expression analysis, RT-PCR
485 was performed using SapphireAmp® Fast PCR Master Mix (Takara; RR350A), while iTaq™ Universal
486 SYBR® Green Supermix (Biorad; 1725121) was used for performing quantitative real-time-PCR. The
487 housekeeping gene *ACT2* was used as an internal control to normalize the target gene expression across
488 samples. All the primers used along with their corresponding gene accession ID are described in **Table**
489 **S1**.

490 Transcriptome analysis was performed with two biological replicates under the described conditions
491 (**Figure S2A**). Paired-end sequencing libraries were prepared using SMART-Seq Library Prep Kit
492 (R40047) as per the manufacturer's protocol and the sequencing was done using Illumina Novaseq 6000
493 S4 platform. Adapter trimming and quality control was performed using FASTP (Chen et al., 2018) and
494 FASTQC (https://www.bioinformatics.babraham.ac.uk/projects/fastqc/) respectively. Kallisto v.0.50.1
495 (Bray et al., 2016) was used for indexing of the reference Arabidopsis transcriptome downloaded from
496 Ensembl. Read mapping was performed using Kallisto following which TxImport (Soneson et al., 2016)
497 was used to read the Kallisto outputs in the R environment. Differential gene expression analysis
498 between control, primed and unprimed seedlings was performed using the edgeR package (Chen et al.,
499 2025) in RStudio. Genes with an adjusted P-value < 0.01 and a cut-off of Log2FC ≥ 1 were used for
500 selecting upregulated genes, and Log2FC ≤ -1 was used for selecting downregulated genes. The
501 expression profiles of the DEGs used for plotting are available as **Dataset S1**.

502 **Protein extraction and Western blot analysis**

503 Soluble protein was extracted from Arabidopsis seedlings as previously described by Yamamoto et al.
504 (2018) with a few modifications. About 40-50 mg of seedlings was collected and frozen in liquid
505 nitrogen. The samples were ground using a Retsch Miller MM400 at 25Hz for 30 seconds (s) (x2
506 cycles). After grinding, 200-300µl of 1x RIPA lysis buffer (Merck; 20-188) containing 10% glycerol,
507 1x phosphatase inhibitor cocktail (PhosSTOP, Roche; 4906837001), and 1x protease inhibitor cocktail
508 (Roche; 4693132001) was added and incubated at 4°C for 1 h at 1500 rpm. The samples were
509 centrifuged at 14000 rpm for 30 min at 4°C, after which the supernatant containing protein was collected
510 and stored at -80°C until further use. Plant protein aggregates were extracted using a standard protocol
511 as described by Phukan et al. (2023).

512 For protein analysis, the protein concentration was estimated using the BCA method, following the
513 manufacturer's instructions (Cat. No. 23225). Protein (20 µg per lane) was loaded onto an 8% SDS-
514 PAGE gel, which was stained with Coomassie Brilliant Blue. Protein bands were visualized after
515 destaining the gel following a standard protocol ("Destaining Solution for Coomassie Brilliant Blue
516 R250," 2007). For Western blot analysis, 20 µg of protein was loaded onto 6-12% SDS-PAGE,
517 following which the proteins were transferred to the nitrocellulose membrane. The blot was blocked
518 using 5% BSA or 2% skim milk solution for 1 h at room temperature (RT), followed by primary
519 antibody incubation (overnight at 4°C). The blot was developed after incubation with secondary
520 antibody (1 h at RT) using Immobilon Forte HRP substrate (Cat. No. WBLUF0500). α-Tub (CST 3873),
521 ATG8 (Abcam, ab77003), ATG8 (Agrisera, AS14 2769), GFP (CST 2956), HSP70 (Abcam, ab2787),
522 HSP90 (Sigma, CA1023), HSP90 (Agrisera, AS08 346), HSP17.6 (Agrisera, AS07 254), HSP21
523 (Agrisera, AS08 285), HSP101 (Agrisera, AS08 287), pS6K (CST 9234), S6K (CST 9202), pAMPK-α
524 (CST 2535), Ubiquitin (CST 3933) and Actin (AS13 2640) were used as primary antibodies. Anti-rabbit
525 (sc-2313; CST 7074) and anti-mouse (CST 7076) were used as secondary antibodies. Blots were
526 quantified densitometrically using the ImageJ software.

527 **Dynamic Light Scattering Measurements**

528 To assess the size distribution profiles, 20 µg of aggregate sample or standard was diluted appropriately
529 in ultrapure water and analyzed using the Litesizer 500 system equipped with a BM10 module (Anton
530 Paar Instruments). Measurements were acquired at 25 °C, using a disposable cuvette and side-scatter
531 detection angle in the automatic mode, with a maximum of 60 runs per sample and 10 s per run.

532 **Statistical Analysis**

533 Data were plotted using GraphPad Prism 10.0 (https://www.graphpad.com/). The experiments were
534 conducted using three biological replicates unless otherwise stated. The data was analysed using One-
535 way ANOVA (for qPCR and phenotype analysis) and Two-way ANOVA (for phenotype analysis) to
536 determine statistical significance. p values <0.05 were considered significant (**Dataset S2 and S3**).

537 **Data Availability**

538 The transcriptome data generated in this study have been deposited to the Sequence Read Archive
539 (SRA) of the National Centre for Biotechnology Information (NCBI) under BioProject ID
540 PRJNA1312973.

541 Acknowledgements

542 MB acknowledges the Council of Scientific and Industrial Research (CSIR), Government of India, for
543 his fellowship. This work was supported by funding from the Department of Science and Technology
544 (Sir JC Bose Fellowship - for BJR), the Science and Engineering Research Board (SPG/2021/004000),
545 and intramural support from IISER Tirupati (ADA and BJR), University of Hyderabad (BJR). We
546 express our sincere gratitude to Prof. Diane Bassham (Iowa State University) and Prof. Federica
547 Brandizzi (Michigan State University) for providing us with seeds of *ire1a ire1b* mutant.

548 Authors Contribution

549 **MB:** Designing the experiments, performing the experiments, interpretation of results, preparation of
550 the figures, writing the manuscript; **ADA:** conceptualization of the research question, supervision of the
551 work, design of the experiments, interpretation of results, writing and editing the manuscript, funding
552 acquisition; **BJR:** conceptualization of the research question, supervision of the work, design of the
553 experiments, interpretation of results, writing and editing the manuscript, funding acquisition.

554 Competing Interests

555 The authors declare no competing interest.

556 References

Baena-González, E., Rolland, F., Thevelein, J. M., & Sheen, J. (2007). A central integrator of transcription networks in plant stress and energy signalling. *Nature 2007 448:7156*, *448*(7156), 938–942. https://doi.org/10.1038/nature06069

Bakery, A., Vraggalas, S., Shalha, B., Chauhan, H., Benhamed, M., & Fragkostefanakis, S. (2024). Heat stress transcription factors as the central molecular rheostat to optimize plant survival and recovery from heat stress. *New Phytologist*, *244*(1), 51–64. https://doi.org/10.1111/NPH.20017

Balmer, A., Pastor, V., Glauser, G., & Mauch-Mani, B. (2018). Tricarboxylates induce defense priming against bacteria in arabidopsis thaliana. *Frontiers in Plant Science*, *9*, 1221. https://doi.org/10.3389/FPLS.2018.01221/BIBTEX

Bao, Y., Pu, Y., Yu, X., Gregory, B. D., Srivastava, R., Howell, S. H., & Bassham, D. C. (2018). IRE1B degrades RNAs encoding proteins that interfere with the induction of autophagy by ER stress in Arabidopsis thaliana. *Autophagy*, *14*(9), 1562–1573. https://doi.org/10.1080/15548627.2018.1462426/SUPPL_FILE/KAUP_A_1462426_SM0835.DOCX

Bäurle, I. (2016). Plant Heat Adaptation: priming in response to heat stress. *F1000Research 2016 5:694*, *5*, 694. https://doi.org/10.12688/f1000research.7526.1

Belda-Palazón, B., Adamo, M., Valerio, C., Ferreira, L. J., Confraria, A., Reis-Barata, D., Rodrigues, A., Meyer, C., Rodriguez, P. L., & Baena-González, E. (2020). A dual function of SnRK2 kinases in the regulation of SnRK1 and plant growth. *Nature Plants 2020 6:11*, *6*(11), 1345–1353. https://doi.org/10.1038/s41477-020-00778-w

Bray, N. L., Pimentel, H., Melsted, P., & Pachter, L. (2016). Near-optimal probabilistic RNA-seq quantification. *Nature Biotechnology*, *34*(5), 525–527. https://doi.org/10.1038/NBT.3519;TECHMETA=45;SUBJMETA=114,2019,212,2785,61,631,794;KWRD=GENOME+INFORMATICS,SOFTWARE,TRANSCRIPTOMICS

Catoni, M., Alvarez-Venegas, R., Worrall, D., Holroyd, G., Barraza, A., Luna, E., Ton, J., & Roberts, M. R. (2022). Long-Lasting Defence Priming by β-Aminobutyric Acid in Tomato Is Marked by Genome-Wide Changes in DNA Methylation. *Frontiers in Plant Science*, *13*, 1071. https://doi.org/10.3389/FPLS.2022.836326/BIBTEX

Chen, S., Zhou, Y., Chen, Y., & Gu, J. (2018). fastp: an ultra-fast all-in-one FASTQ preprocessor. *Bioinformatics*, *34*(17), i884–i890. https://doi.org/10.1093/BIOINFORMATICS/BTY560

Chen, Y., Aung, K., Rolčík, J., Walicki, K., Friml, J., & Brandizzi, F. (2013). INTER-REGULATION OF THE UNFOLDED PROTEIN RESPONSE AND AUXIN SIGNALING. *The Plant Journal : For Cell and Molecular Biology*, *77*(1), 97. https://doi.org/10.1111/TPJ.12373

Chen, Y., Chen, L., Lun, A. T. L., Baldoni, P. L., & Smyth, G. K. (2025). edgeR v4: powerful differential analysis of sequencing data with expanded functionality and improved support for small counts and larger datasets. *Nucleic Acids Research*, *53*(2). https://doi.org/10.1093/NAR/GKAF018

Conrath, U., Beckers, G. J. M., Flors, V., García-Agustín, P., Jakab, G., Mauch, F., Newman, M. A., Pieterse, C. M. J., Poinssot, B., Pozo, M. J., Pugin, A., Schaffrath, U., Ton, J., Wendehenne, D.,

Zimmerli, L., & Mauch-Mani, B. (2007). Priming: Getting Ready for Battle. *Http://Dx.Doi.Org/10.1094/MPMI-19-1062*, *19*(10), 1062–1071. https://doi.org/10.1094/MPMI-19-1062

Crespo-Salvador, Ó., Escamilla-Aguilar, M., López-Cruz, J., López-Rodas, G., & González-Bosch, C. (2018). Determination of histone epigenetic marks in Arabidopsis and tomato genes in the early response to Botrytis cinerea. *Plant Cell Reports*, *37*(1), 153–166. https://doi.org/10.1007/S00299-017-2218-9/FIGURES/6

Dannfald, A., Carpentier, M.-C., Merret, R., Favory, J.-J., & Deragon, J.-M. (2025). Plant response to intermittent heat stress involves modulation of mRNA translation efficiency. *Plant Physiology*, *197*(2), 648. https://doi.org/10.1093/PLPHYS/KIAE648

Deng, Y., Humbert, S., Liu, J. X., Srivastava, R., Rothstein, S. J., & Howell, S. H. (2011). Heat induces the splicing by IRE1 of a mRNA encoding a transcription factor involved in the unfolded protein response in Arabidopsis. *Proceedings of the National Academy of Sciences of the United States of America*, *108*(17), 7247–7252. https://doi.org/10.1073/PNAS.1102117108/SUPPL_FILE/PNAS.201102117SI.PDF

Deng, Y., Srivastava, R., & Howell, S. H. (2013). Protein kinase and ribonuclease domains of IRE1 confer stress tolerance, vegetative growth, and reproductive development in Arabidopsis. *Proceedings of the National Academy of Sciences of the United States of America*, *110*(48), 19633–19638. https://doi.org/10.1073/PNAS.1314749110/SUPPL_FILE/PNAS.201314749SI.PDF

Destaining solution for Coomassie brilliant blue R250. (2007). *Cold Spring Harbor Protocols*, *2007*(2), pdb.rec10717. https://doi.org/10.1101/PDB.REC10717

Duan, Z., Chen, K., Yang, T., You, R., Chen, B., Li, J., & Liu, L. (2023). Mechanisms of Endoplasmic Reticulum Protein Homeostasis in Plants. *International Journal of Molecular Sciences 2023, Vol. 24, Page 17599*, *24*(24), 17599. https://doi.org/10.3390/IJMS242417599

Espinas, N. A., Saze, H., & Saijo, Y. (2016). Epigenetic control of defense signaling and priming in plants. *Frontiers in Plant Science*, *7*(AUG2016), 1201. https://doi.org/10.3389/FPLS.2016.01201/BIBTEX

Fahad, S., Bajwa, A. A., Nazir, U., Anjum, S. A., Farooq, A., Zohaib, A., Sadia, S., Nasim, W., Adkins, S., Saud, S., Ihsan, M. Z., Alharby, H., Wu, C., Wang, D., & Huang, J. (2017). Crop production under drought and heat stress: Plant responses and management options. *Frontiers in Plant Science*, *8*, 1147. https://doi.org/10.3389/FPLS.2017.01147/BIBTEX

Friedrich, T., Oberkofler, V., Trindade, I., Altmann, S., Brzezinka, K., Lämke, J., Gorka, M., Kappel, C., Sokolowska, E., Skirycz, A., Graf, A., & Bäurle, I. (2021). Heteromeric HSFA2/HSFA3 complexes drive transcriptional memory after heat stress in Arabidopsis. *Nature Communications*, *12*(1). https://doi.org/10.1038/s41467-021-23786-6

Gamir, J., Sánchez-Bel, P., & Flors, V. (2014). Molecular and physiological stages of priming: how plants prepare for environmental challenges. *Plant Cell Reports*, *33*(12), 1935–1949. https://doi.org/10.1007/S00299-014-1665-9

631 Gao, C., Peng, X., Zhang, L., Zhao, Q., Ma, L., Yu, Q., Lian, X., Gao, L., Xiong, L., & Li, S. (2023).
632 Proteome and Ubiquitylome Analyses of Maize Endoplasmic Reticulum under Heat Stress. *Genes*,
633 *14*(3), 749. https://doi.org/10.3390/GENES14030749/S1

634 Gulen, H., & Eris, A. (2004). Effect of heat stress on peroxidase activity and total protein content in
635 strawberry plants. *Plant Science*, *166*(3), 739–744. https://doi.org/10.1016/J.PLANTSCI.2003.11.014

636 Hartl, F. U., Bracher, A., & Hayer-Hartl, M. (2011). Molecular chaperones in protein folding and
637 proteostasis. *Nature*, *475*(7356), 324–332. https://doi.org/10.1038/nature10317

638 Huang, X., Yao, J., Liu, L., Luo, Y., & Yang, A. (2022). Atg8–PE protein-based in vitro biochemical
639 approaches to autophagy studies. *Autophagy*, *18*(9), 2020.
640 https://doi.org/10.1080/15548627.2022.2025572

641 Humbert, S., Zhong, S., Deng, Y., Howell, S. H., & Rothstein, S. J. (2012). Alteration of the bZIP60/IRE1
642 Pathway Affects Plant Response to ER Stress in Arabidopsis thaliana. *PLOS ONE*, *7*(6), e39023.
643 https://doi.org/10.1371/JOURNAL.PONE.0039023

644 Jung, H., Lee, H. N., Marshall, R. S., Lomax, A. W., Yoon, M. J., Kim, J., Kim, J. H., Vierstra, R. D., &
645 Chung, T. (2020). Arabidopsis cargo receptor NBR1 mediates selective autophagy of defective
646 proteins. *Journal of Experimental Botany*, *71*(1), 73–89. https://doi.org/10.1093/JXB/ERZ404

647 Kang, S., Shin, K. D., Kim, J. H., & Chung, T. (2018). Autophagy-related (ATG) 11, ATG9 and the
648 phosphatidylinositol 3-kinase control ATG2-mediated formation of autophagosomes in Arabidopsis.
649 *Plant Cell Reports*, *37*(4), 653–664. https://doi.org/10.1007/s00299-018-2258-9

650 Kotkar, H., & Giri, A. (2020). Plant epigenetics and the 'intelligent' priming system to combat biotic stress.
651 *Epigenetics of the Immune System*, 25–38. https://doi.org/10.1016/B978-0-12-817964-2.00002-2

652 Li, Z., & Howell, S. H. (2021). Review: The two faces of IRE1 and their role in protecting plants from
653 stress. *Plant Science*, *303*, 110758. https://doi.org/10.1016/J.PLANTSCI.2020.110758

654 Liu, H., Able, A. J., & Able, J. A. (2022). Priming crops for the future: rewiring stress memory. *Trends in*
655 *Plant Science*, *27*(7), 699–716. https://doi.org/10.1016/j.tplants.2021.11.015

656 Liu, Y., Burgos, J. S., Deng, Y., Srivastava, R., Howell, S. H., & Bassham, D. C. (2012). Degradation of the
657 endoplasmic reticulum by autophagy during endoplasmic reticulum stress in Arabidopsisc w. *Plant*
658 *Cell*, *24*(11), 4635–4651. https://doi.org/10.1105/tpc.112.101535

659 Lobell, D. B., Sibley, A., & Ivan Ortiz-Monasterio, J. (2012). Extreme heat effects on wheat senescence in
660 India. *Nature Climate Change 2012 2:3*, *2*(3), 186–189. https://doi.org/10.1038/nclimate1356

661 Löchli, K., Torbica, E., Haile-Weldeslasie, M., Baku, D., Aziz, A., Bublak, D., & Fragkostefanakis, S.
662 (2023). Crosstalk between endoplasmic reticulum and cytosolic unfolded protein response in tomato.
663 *Cell Stress and Chaperones*, *28*(5), 511–528. https://doi.org/10.1007/s12192-022-01316-7

664 Long, S. P., & Ort, D. R. (2010). More than taking the heat: crops and global change. *Current Opinion in*
665 *Plant Biology*, *13*(3), 240–247. https://doi.org/10.1016/J.PBI.2010.04.008

666 Marshall, R. S., & Vierstra, R. D. (2018). Autophagy: The Master of Bulk and Selective Recycling. *Annual*
667 *Review of Plant Biology*, *69*(Volume 69, 2018), 173–208. https://doi.org/10.1146/ANNUREV-
668 ARPLANT-042817-040606/CITE/REFWORKS

669 Maurel, M., Chevet, E., Tavernier, J., & Gerlo, S. (2014). Getting RIDD of RNA: IRE1 in cell fate
670 regulation. *Trends in Biochemical Sciences*, *39*(5), 245–254.
671 https://doi.org/10.1016/J.TIBS.2014.02.008

672 McLoughlin, F., Kim, M., Marshall, R. S., Vierstra, R. D., & Vierling, E. (2019). HSP101 Interacts with the
673 Proteasome and Promotes the Clearance of Ubiquitylated Protein Aggregates. *Plant Physiology*,
674 *180*(4), 1829–1847. https://doi.org/10.1104/PP.19.00263

675 Mesihovic, A., Ullrich, S., Rosenkranz, R. R. E., Gebhardt, P., Bublak, D., Eich, H., Weber, D., Berberich,
676 T., Scharf, K. D., Schleiff, E., & Fragkostefanakis, S. (2022). HsfA7 coordinates the transition from
677 mild to strong heat stress response by controlling the activity of the master regulator HsfA1a in tomato.
678 *Cell Reports*, *38*(2), 110224. https://doi.org/10.1016/J.CELREP.2021.110224

679 Minina, E. A., Filonova, L. H., Fukada, K., Savenkov, E. I., Gogvadze, V., Clapham, D., Sanchez-Vera, V.,
680 Suarez, M. F., Zhivotovsky, B., Daniel, G., Smertenko, A., & Bozhkov, P. V. (2013). Autophagy and
681 metacaspase determine the mode of cell death in plants. *Journal of Cell Biology*, *203*(6), 917–927.
682 https://doi.org/10.1083/JCB.201307082

683 Mittler, R., Finka, A., & Goloubinoff, P. (2012). How do plants feel the heat? *Trends in Biochemical*
684 *Sciences*, *37*(3), 118–125. https://doi.org/10.1016/J.TIBS.2011.11.007

685 Mogk, A., Bukau, B., & Kampinga, H. H. (2018). Cellular Handling of Protein Aggregates by
686 Disaggregation Machines. *Molecular Cell*, *69*(2), 214–226.
687 https://doi.org/10.1016/J.MOLCEL.2018.01.004

688 Nagy-Réder, D., Birinyi, Z., Rakszegi, M., Békés, F., & Gell, G. (2022). The effect of abiotic stresses on the
689 protein composition of four hungarian wheat varieties. *Plants*, *11*(1), 1.
690 https://doi.org/10.3390/PLANTS11010001/S1

691 Nair, A. U., Prasad, D., Bhukya, N., Sunkar, R., Chavali, S., Allu, A. D., & Noctor, G. (2022). Molecular
692 basis of priming-induced acquired tolerance to multiple abiotic stresses in plants. *Journal of*
693 *Experimental Botany*, *73*(11), 3355–3371. https://doi.org/10.1093/JXB/ERAC089

694 Nawkar, G. M., Lee, E. S., Shelake, R. M., Park, J. H., Ryu, S. W., Kang, C. H., & Lee, S. Y. (2018).
695 Activation of the transducers of unfolded protein response in plants. *Frontiers in Plant Science*, *9*, 214.
696 https://doi.org/10.3389/FPLS.2018.00214/BIBTEX

697 Noh, S. W., Seo, R.-R., Park, H. J., & Jung, H. W. (2021). Two Arabidopsis Homologs of Human Lysine-
698 Specific Demethylase Function in Epigenetic Regulation of Plant Defense Responses. *Frontiers in*
699 *Plant Science*, *0*, 1133. https://doi.org/10.3389/FPLS.2021.688003

700 Ohama, N., Sato, H., Shinozaki, K., & Yamaguchi-Shinozaki, K. (2017). Transcriptional Regulatory
701 Network of Plant Heat Stress Response. In *Trends in Plant Science* (Vol. 22, Issue 1, pp. 53–65).
702 Elsevier Ltd. https://doi.org/10.1016/j.tplants.2016.08.015

Pastor-Cantizano, N., Ko, D. K., Angelos, E., Pu, Y., & Brandizzi, F. (2020). Functional Diversification of ER Stress Responses in Arabidopsis. *Trends in Biochemical Sciences*, *45*(2), 123–136. https://doi.org/10.1016/J.TIBS.2019.10.008

Phukan, U. J., Stael, S., Gonçalves, A., Van Breusegem, F., & Coll, N. S. (2023). Detection and Quantification of Protein Aggregates in Plants. In *Methods in Molecular Biology* (Vol. 2581, pp. 221–228). Humana Press Inc. https://doi.org/10.1007/978-1-0716-2784-6_15

Pu, Y., Luo, X., & Bassham, D. C. (2017). Tor-dependent and -independent pathways regulate autophagy in arabidopsis thaliana. *Frontiers in Plant Science*, *8*, 1204. https://doi.org/10.3389/FPLS.2017.01204/BIBTEX

Pu, Y., Ruberti, C., Angelos, E. R., & Brandizzi, F. (2019). AtIRE1C, an unconventional isoform of the UPR master regulator AtIRE1, is functionally associated with AtIRE1B in Arabidopsis gametogenesis. *Plant Direct*, *3*(11). https://doi.org/10.1002/pld3.187

Raffeiner, M., Zhu, S., González-Fuente, M., & Üstün, S. (2023). Interplay between autophagy and proteasome during protein turnover. *Trends in Plant Science*, *28*(6), 698–714. https://doi.org/10.1016/J.TPLANTS.2023.01.013

Richter, K., Haslbeck, M., & Buchner, J. (2010). The Heat Shock Response: Life on the Verge of Death. *Molecular Cell*, *40*(2), 253–266. https://doi.org/10.1016/J.MOLCEL.2010.10.006/ASSET/54785DAF-4BAF-48EF-9C3C-98716B4FC179/MAIN.ASSETS/GR3.JPG

Rosenzweig, R., Nillegoda, N. B., Mayer, M. P., & Bukau, B. (2019). The Hsp70 chaperone network. *Nature Reviews Molecular Cell Biology 2019 20:11*, *20*(11), 665–680. https://doi.org/10.1038/s41580-019-0133-3

Samantaray, D., Vankanavath, A. B., Kadumuri, R. V., Ramadurai, D., Chavali, S., & Allu, A. D. (2023). Thermopriming mitigates the effects of heat stress by modulating the expression of Heat shock factors in Brassica juncea (Indian mustard). *Environmental and Experimental Botany*, *211*, 105371. https://doi.org/10.1016/J.ENVEXPBOT.2023.105371

Schmitt, J., Offermann, F., Söder, M., Frühauf, C., & Finger, R. (2022). Extreme weather events cause significant crop yield losses at the farm level in German agriculture. *Food Policy*, *112*, 102359. https://doi.org/10.1016/J.FOODPOL.2022.102359

Schneider, C. A., Rasband, W. S., & Eliceiri, K. W. (2012). NIH Image to ImageJ: 25 years of image analysis. In *Nature Methods* (Vol. 9, Issue 7, pp. 671–675). https://doi.org/10.1038/nmeth.2089

Sedaghatmehr, M., Mueller-Roeber, B., & Balazadeh, S. (2016). The plastid metalloprotease FtsH6 and small heat shock protein HSP21 jointly regulate thermomemory in Arabidopsis. *Nature Communications*, *7*. https://doi.org/10.1038/NCOMMS12439

Sedaghatmehr, M., Thirumalaikumar, V. P., Kamranfar, I., Marmagne, A., Masclaux-Daubresse, C., & Balazadeh, S. (2019). A regulatory role of autophagy for resetting the memory of heat stress in plants. *Plant, Cell & Environment*, *42*(3), 1054–1064. https://doi.org/10.1111/PCE.13426

739 Sedaghatmehr, M., Thirumalaikumar, V. P., Kamranfar, I., Schulz, K., Mueller-Roeber, B., Sampathkumar,
740 A., & Balazadeh, S. (2021). Autophagy complements metalloprotease FtsH6 in degrading plastid heat
741 shock protein HSP21 during heat stress recovery. *Journal of Experimental Botany*, *72*(21), 7498–7513.
742 https://doi.org/10.1093/jxb/erab304

743 Selinski, J., Frings, S., & Schmidt-Schippers, R. (2024). Perception and processing of stress signals by plant
744 mitochondria. *The Plant Journal*, *120*(6), 2337. https://doi.org/10.1111/TPJ.17133

745 Serrano, N., Ling, Y., Bahieldin, A., & Mahfouz, M. M. (2019). Thermopriming reprograms metabolic
746 homeostasis to confer heat tolerance. *Scientific Reports 2019 9:1*, *9*(1), 1–14.
747 https://doi.org/10.1038/s41598-018-36484-z

748 Sharma, I., Talakayala, A., Tiwari, M., Asinti, S., & Kirti, P. B. (2024). A synchronized symphony:
749 Intersecting roles of ubiquitin proteasome system and autophagy in cellular degradation. *Plant*
750 *Physiology and Biochemistry*, *212*, 108700. https://doi.org/10.1016/J.PLAPHY.2024.108700

751 Shin, K. D., Lee, H. N., & Chung, T. (2014). A revised assay for monitoring autophagic flux in Arabidopsis
752 Thaliana reveals involvement of autophagy-related9 in autophagy. *Molecules and Cells*, *37*(5), 399–
753 405. https://doi.org/10.14348/molcells.2014.0042

754 Signorelli, S., Tarkowski, Ł. P., Van den Ende, W., & Bassham, D. C. (2019). Linking Autophagy to Abiotic
755 and Biotic Stress Responses. *Trends in Plant Science*, *24*(5), 413–430.
756 https://doi.org/10.1016/J.TPLANTS.2019.02.001

757 Sjøgaard, I. M. Z., Bressendorff, S., Prestel, A., Kausika, S., Oksbjerg, E., Kragelund, B. B., & Brodersen,
758 P. (2019). The transmembrane autophagy cargo receptors ATI1 and ATI2 interact with ATG8 through
759 intrinsically disordered regions with distinct biophysical properties. *Biochemical Journal*, *476*(3), 449–
760 465. https://doi.org/10.1042/BCJ20180748

761 Soneson, C., Love, M. I., & Robinson, M. D. (2016). Differential analyses for RNA-seq: transcript-level
762 estimates improve gene-level inferences. *F1000Research 2016 4:1521*, *4*, 1521.
763 https://doi.org/10.12688/f1000research.7563.2

764 Song, G. C., Choi, H. K., & Ryu, C. M. (2015). Gaseous 3-pentanol primes plant immunity against a
765 bacterial speck pathogen, pseudomonas syringae pv. Tomato via salicylic acid and jasmonic acid-
766 dependent signaling pathways in arabidopsis. *Frontiers in Plant Science*, *6*(OCTOBER), 1–7.
767 https://doi.org/10.3389/fpls.2015.00821

768 Soto-Burgos, J., & Bassham, D. C. (2017). SnRK1 activates autophagy via the TOR signaling pathway in
769 Arabidopsis thaliana. *PLOS ONE*, *12*(8), e0182591.
770 https://doi.org/10.1371/JOURNAL.PONE.0182591

771 Su, T., Li, X., Yang, M., Shao, Q., Zhao, Y., Ma, C., & Wang, P. (2020). Autophagy: An Intracellular
772 Degradation Pathway Regulating Plant Survival and Stress Response. *Frontiers in Plant Science*, *11*,
773 164. https://doi.org/10.3389/FPLS.2020.00164/BIBTEX

774 Sun, J. L., Li, J. Y., Wang, M. J., Song, Z. T., & Liu, J. X. (2021). Protein Quality Control in Plant
775 Organelles: Current Progress and Future Perspectives. *Molecular Plant*, *14*(1), 95–114.

https://doi.org/10.1016/J.MOLP.2020.10.011/ASSET/6AEADDB2-BAD0-424B-915F-7ABEC2E3C31F/MAIN.ASSETS/GR4.JPG

Suttangkakul, A., Li, F., Chung, T., & Vierstra, R. D. (2011). The ATG1/ATG13 protein kinase complex is both a regulator and a target of autophagic recycling in Arabidopsis. *The Plant Cell*, *23*(10), 3761–3779. https://doi.org/10.1105/TPC.111.090993

Thirumalaikumar, V. P., Gorka, M., Schulz, K., Masclaux-Daubresse, C., Sampathkumar, A., Skirycz, A., Vierstra, R. D., & Balazadeh, S. (2020). Selective autophagy regulates heat stress memory in Arabidopsis by NBR1-mediated targeting of HSP90.1 and ROF1. *Autophagy*, *17*(9), 2184–2199. https://doi.org/10.1080/15548627.2020.1820778

Tugizimana, F., Mhlongo, M. I., Piater, L. A., & Dubery, I. A. (2018). Metabolomics in Plant Priming Research: The Way Forward? *International Journal of Molecular Sciences*, *19*(6). https://doi.org/10.3390/IJMS19061759

Upadhyaya, S., Agrawal, S., Gorakshakar, A., & Rao, B. J. (2020). TOR kinase activity in Chlamydomonas reinhardtii is modulated by cellular metabolic states. *FEBS Letters*, *594*(19), 3122–3141. https://doi.org/10.1002/1873-3468.13888

Wang, P., Nolan, T. M., Yin, Y., & Bassham, D. C. (2020). Identification of transcription factors that regulate ATG8 expression and autophagy in Arabidopsis. *Autophagy*, *16*(1), 123–139. https://doi.org/10.1080/15548627.2019.1598753;SUBPAGE:STRING:FULL

Wang, X., Tan, N. W. K., Chung, F. Y., Yamaguchi, N., Gan, E. S., & Ito, T. (2023). Transcriptional Regulators of Plant Adaptation to Heat Stress. In *International Journal of Molecular Sciences* (Vol. 24, Issue 17). Multidisciplinary Digital Publishing Institute (MDPI). https://doi.org/10.3390/ijms241713297

Wang, Y., Cai, S., Yin, L., Shi, K., Xia, X., Zhou, Y., Yu, J., & Zhou, J. (2015). Tomato HsfA1a plays a critical role in plant drought tolerance by activating ATG genes and inducing autophagy. *Autophagy*, *11*(11), 2033–2047. https://doi.org/10.1080/15548627.2015.1098798

Wilkinson, S. W., Mageroslashy, M. H., Lopez Sanchez, A., Smith, L. M., Furci, L., Cotton, T. E. A., Krokene, P., & Ton, J. (2019). Surviving in a Hostile World: Plant Strategies to Resist Pests and Diseases. *Https://Doi.Org/10.1146/Annurev-Phyto-082718-095959*, *57*, 505–529. https://doi.org/10.1146/ANNUREV-PHYTO-082718-095959

Xie, D. L., Huang, H. M., Zhou, C. Y., Liu, C. X., Kanwar, M. K., Qi, Z. Y., & Zhou, J. (2022). HsfA1a confers pollen thermotolerance through upregulating antioxidant capacity, protein repair, and degradation in Solanum lycopersicum L. *Horticulture Research*, *9*. https://doi.org/10.1093/hr/uhac163

Yamamoto, T., Hoshikawa, K., Ezura, K., Okazawa, R., Fujita, S., Takaoka, M., Mason, H. S., Ezura, H., & Miura, K. (2018). Improvement of the transient expression system for production of recombinant proteins in plants. *Scientific Reports 2018 8:1*, *8*(1), 1–10. https://doi.org/10.1038/s41598-018-23024-y

811 Yang, C., Li, X., Yang, L., Chen, S., Liao, J., Li, K., Zhou, J., Shen, W., Zhuang, X., Bai, M., Bassham, D.
812 C., & Gao, C. (2023). A positive feedback regulation of SnRK1 signaling by autophagy in plants.
813 *Molecular Plant*. https://doi.org/10.1016/J.MOLP.2023.07.001

814 Yang, X., Srivastava, R., Howell, S. H., & Bassham, D. C. (2016). Activation of autophagy by unfolded
815 proteins during endoplasmic reticulum stress. *Plant Journal*, *85*(1), 83–95.
816 https://doi.org/10.1111/tpj.13091

817 Ye, M., Glauser, G., Lou, Y., Erb, M., & Hu, L. (2019). Molecular Dissection of Early Defense Signaling
818 Underlying Volatile-Mediated Defense Regulation and Herbivore Resistance in Rice. *The Plant Cell*,
819 *31*(3), 687–698. https://doi.org/10.1105/TPC.18.00569

820 Yoo, J. Y., Ko, K. S., Vu, B. N., Lee, Y. E., Choi, H. N., Lee, Y. N., Fanata, W. I. D., Harmoko, R., Lee, S.
821 K., Chung, W. S., Hong, J. C., & Lee, K. O. (2024). IRE1 is implicated in protein synthesis regulation
822 under ER stress conditions in plants. *Plant Physiology and Biochemistry*, *215*, 108963.
823 https://doi.org/10.1016/J.PLAPHY.2024.108963

824 Yoshida, T., Ohama, N., Nakajima, J., Kidokoro, S., Mizoi, J., Nakashima, K., Maruyama, K., Kim, J. M.,
825 Seki, M., Todaka, D., Osakabe, Y., Sakuma, Y., SchöZ, F., Shinozaki, K., & Yamaguchi-Shinozaki, K.
826 (2011). Arabidopsis HsfA1 transcription factors function as the main positive regulators in heat shock-
827 responsive gene expression. *Molecular Genetics and Genomics*, *286*(5–6), 321–332.
828 https://doi.org/10.1007/s00438-011-0647-7

829 Zhou, J., Wang, J., Cheng, Y., Chi, Y. J., Fan, B., Yu, J. Q., & Chen, Z. (2013). NBR1-Mediated Selective
830 Autophagy Targets Insoluble Ubiquitinated Protein Aggregates in Plant Stress Responses. *PLoS*
831 *Genetics*, *9*(1). https://doi.org/10.1371/journal.pgen.1003196

832 Zhou, J., Wang, J., Yu, J. Q., & Chen, Z. (2014). Role and regulation of autophagy in heat stress responses
833 of tomato plants. *Frontiers in Plant Science*, *5*(APR), 82255.
834 https://doi.org/10.3389/FPLS.2014.00174/BIBTEX

835 Zhou, J., Wang, Z., Wang, X., Li, X., Zhang, Z., Fan, B., Zhu, C., & Chen, Z. (2018). Dicot-specific ATG8-
836 interacting ATI3 proteins interact with conserved UBAC2 proteins and play critical roles in plant stress
837 responses. *Autophagy*, *14*(3), 487–504. https://doi.org/10.1080/15548627.2017.1422856

838

839 Figure Legends

840 **Figure 1: Priming improves survival under severe heat stress.** (A) The experimental paradigm is
841 schematised where 37°C was used as a priming stimulus, followed by recovery at 22°C (optimal growth
842 temperature), and then exposed to a 45°C heat-triggering stimulus for the indicated time durations. Control
843 (untreated) and unprimed seedlings (subjected to only 45°C) were compared in parallel. (B) Post-heat
844 stress, seedlings were monitored over multiple days at 22°C to assess their recovery. The panel depicts
845 representative images for primed, unprimed and control conditions. Scale bar, 0.5cm. The growth recovery
846 was quantified based on (C) the number of leaves per plant (n=3 biological replicates, with 16 seedlings

per replicate), (D) root length (n=3 biological replicates, with 6 seedlings per replicate), and (E) fresh weight (n=3 biological replicates, with 16 seedlings pooled per replicate) at the indicated time points. Despite an initial halt in growth (as observed in root length), primed seedlings resumed growth similar to the control, whereas unprimed plants exhibited complete growth arrest and ultimately failed to survive. Data are presented as mean ± SEM (for leaves per plant) and mean ± SD (for root length and fresh weight). Statistical significance was determined using two-way ANOVA, where the asterisk (** $p < 0.01$; **** $p < 0.0001$) indicates significant differences between the primed and unprimed seedlings.

Figure 2: Priming leads to an increase in chaperone abundance post-heat stress via HSFA1. (A) The schematics of the experimental paradigm is shown. AP, BT, and 0-3 DPS denote the time points at which seedlings were collected (PS-Priming Stimulus, TS-Triggering Stimulus). (B) Misfolded protein accumulation following heat stress was determined by checking for the presence of *bZIP60* spliced form (*bZIP60s*). Expression analysis suggested that primed seedlings initially accumulated misfolded proteins but recovered by 1 DPS, whereas unprimed seedlings experienced a sustained accumulation of misfolded proteins (n=3 biological replicates). Statistical significance was calculated using one-way ANOVA (**** $p < 0.0001$; *** $p < 0.001$; ns – not significant). (C) Illustrated representation of the processes involved in the maintenance of protein homeostasis. (D-G) To assess the status of HSR, western blot analysis of HSP17.6, HSP21, HSP70, HSP90, and HSP101 proteins in various samples was performed post-heat stress. The data revealed that priming led to an increase in the abundance of HSPs, which persisted even after stress removal. In contrast, unprimed seedlings did not show any increase in HSP abundance compared with the control (n=3 biological replicates). α-Tubulin served as a loading control. (H) Heat map showing the mean expression levels of *HSPs* across different time points, derived from transcriptome data (n=2 biological replicates). The data suggests that priming stimulus led to an increase in *HSP* levels compared to control. Unprimed seedlings also displayed an increase in *HSP* abundance post-stress compared to control, but the level remained lower than that of primed seedlings. (I) The panel depicts representative images of *hsfa1a/b/d* (referred to as *a/b/d*), Col-0 and Ws-0 post-priming/triggering heat stress. The effect of priming on heat stress response was lost in the *a/b/d* mutant compared to Col-0/Ws-0. Unprimed *a/b/d* failed to survive, similar to that of Col-0/Ws-0 post-heat stress (n=3 biological replicates). (J) Immunoblot analysis of HSPs revealed that primed-WT displayed an increased abundance post-priming, whereas primed *a/b/d* failed to display HSP abundance (n=3 biological replicates).

Figure 3: Priming stimulus activates the transcriptional unfolded protein response, while loss of UPR delays seedling recovery post-heat stress. (A) Transcriptome data was used to assess unfolded protein response (UPR) following heat stress. The heatmap displays the mean expression levels of genes involved in endoplasmic reticulum (ER) quality control (ERQC) and ER-associated degradation (ERAD), representing two major branches of the UPR pathway. Primed seedlings exhibited enhanced activation of UPR genes compared to control, whereas unprimed seedlings fail to induce a comparable response following heat stress. (B) Panel depicts representative images of UPR mutants, *bzip60* and *ire1a/b* lines, post-priming/triggering heat stress. Primed *bzip60* and *ire1a/b* knockout mutants survived severe heat stress, whereas the unprimed seedlings failed to survive (n=3 biological replicates). (C-D) Primary root length and fresh weight were quantified at 7 DPS across all genotypes. For WT, primed seedlings showed

886 comparable root length to control, whereas, primed *bzip60* and *ire1a/b* mutants showed a significant
887 reduction in root length compared to their respective controls. Fresh weight was found to be reduced in
888 primed seedlings of all genotypes when compared to their respective control. On the x-axis, C denotes
889 control and P denotes primed seedlings. Data are presented as median ± SD (n=3 biological replicates,
890 comprising a total of 15-24 seedlings represented as individual grey circles). Statistical significance was
891 assessed using one-way ANOVA followed by Tukey's post-hoc test. Compact letter display was used to
892 denote statistically significant differences among groups ($p < 0.05$); groups not sharing a common letter
893 are significantly different. (E) To assess the HSR status in *bzip60* and *ire1a/b* mutants, western blot
894 analysis of HSP17.6, HSP21, HSP70, HSP90, and HSP101 proteins was performed for all the conditions
895 post-heat stress. The data revealed that priming led to an increase in the abundance of HSPs in *bzip60* and
896 *ire1a/b*, which persisted even after the stress removal, indicating an active HSR in the mutants. Unprimed
897 *bzip60* and *ire1a/b* seedlings did not show any increase in HSP levels, similar to unprimed wild-type (n=3
898 biological replicates). [AP - After priming; AT - After triggering (Day 0); DPS - Days post-stress].

899 **Figure 4: Primed seedlings display temporary autophagy, whereas unprimed seedlings experience**
900 **sustained autophagy.** (A) The heat map shows the mean expression levels of differentially expressed
901 autophagy-related genes (ATGs) across time points, derived from transcriptome analysis. The data
902 indicate that the priming stimulus leads to an increase in the expression of ATGs compared to the control.
903 (B-C) Western blot analysis of ATG8 revealed that primed seedlings showed slightly induced autophagy
904 (as seen by ATG8-PE levels) compared to control at the AP time point, which increased further post-
905 triggering stress (0h to 4h). However, at 1 DPS, autophagy in primed is comparable to control levels. In
906 contrast, unprimed seedlings displayed a surge in the ATG8-PE levels post-stress (0h) that remained
907 continuously higher compared to the control. Numbers below denote intensity values post-normalisation
908 with respect to the corresponding control time point (n=3 biological replicates). (D) Western blot of GFP-
909 ATG8 and free-GFP (both detected using anti-GFP antibody) for various samples at the post-heat stress
910 time points revealed that autophagy flux in unprimed seedlings remained high during the stress recovery
911 period, as seen by the high free-GFP levels, whereas autophagy in primed seedlings was similar to that of
912 the control. Numbers below represent normalised mean intensity of free-GFP/Total-GFP (GFP-
913 ATG8+free-GFP) with respect to the corresponding control time point (n=2 biological replicates). (E)
914 Expression of autophagy inhibitors *BGLU21* and *PR-14* is represented as fold change compared to control.
915 In primed, expression of autophagy inhibitors was found to be downregulated at AP, BT and AT
916 timepoints, but it returned to control levels by 1 DPS. However, in unprimed, autophagy inhibitors were
917 continuously maintained at lower levels post-stress. The data are presented as mean ± SD (n=2/3 biological
918 replicates). Statistical significance was calculated using one-way ANOVA (**** $p < 0.0001$; *** $p < 0.001$;
919 ** $p < 0.01$; ns - not significant). (F) Data-driven illustrated representation depicting the correlation
920 between the downregulation of the autophagy inhibitor *BGLU21* coinciding with the induction of ATG8
921 levels in primed and unprimed seedlings. [AP - After priming; BT - Before triggering; AT - After
922 triggering (Day 0); DPS - Days post-stress].

923 **Figure 5: Impairment of the heat shock response amplifies autophagy during proteotoxic stress.** (A)
924 Western blot analysis of ATG8 in *hsfa1a/b/d* mutants shows that autophagy remains highly induced in

both primed and unprimed following heat stress (n=3 biological replicates). The numbers below denote intensity values post-normalisation with respect to corresponding control timepoint. (B) Data-driven illustrated line plots comparing ATG8 and HSP abundance profiles in primed WT, primed *hsfa1a/b/d*, and unprimed seedlings at the indicated timepoints. The bar plots above indicate the percentage of seedling survival at 7 DPS (n=3 biological replicates per condition). In primed WT, chaperone accumulation (HSPs) peaks early and is accompanied by transient ATG8 induction, suggesting efficient proteostasis and resolution of stress via timely attenuation of autophagy. Conversely, both unprimed WT and primed *hsfa1a/b/d* mutants failed to induce HSPs, correlating with sustained ATG8 accumulation and complete post-stress mortality. Collectively, these data illustrate that thermotolerance is driven by a coordinated HSP-autophagy interplay, whereas its failure leads to autophagy overactivation and seedling lethality. [DPS - Days post stress].

Figure 6: Priming facilitates effective aggregate clearance following heat stress. (A) Immunoblot analysis of ubiquitin-conjugated aggregates shows that unprimed seedlings have a higher accumulation of aggregates compared to primed and control seedlings by 1 DPS. Box plot represents the normalised mean intensity for ubiquitin in the insoluble fraction. The dotted line denotes the control value (n=2 biological replicates). (B) Dynamic Light Scattering (DLS) analysis showing the particle size distribution of protein aggregates isolated at 1 DPS from control, primed, and unprimed seedlings. Bovine serum albumin (BSA) was used as a monomeric protein standard. Unprimed seedlings accumulated a higher proportion of large aggregates (460.1 nm and 6662.6 nm), indicating extensive aggregation. In contrast, primed seedlings displayed smaller aggregate populations (174.1 nm and 1977.0 nm), comparable to control, suggesting more efficient aggregate clearance. (C) Autocorrelation function (g^2) curves derived from DLS measurements reflect particle size dynamics and diffusion behavior. BSA exhibited the steepest/fastest decay, consistent with uniform small particles. Aggregates derived from unprimed seedlings exhibited the slowest decay, reflective of larger, less diffusive aggregate populations. Primed samples show a faster decay than unprimed, indicating smaller and more dynamic aggregates. Data is representative of two biological replicates.

Figure 7: Priming-mediated acquired thermotolerance underlies dynamic regulation of proteostasis. The illustration compares the responses of primed (top panel) and unprimed (bottom panel) Arabidopsis seedlings upon exposure to severe heat stress. In primed seedlings, HSFA1-mediated transcriptional activation drives a robust heat shock response (HSR) associated with accumulation of HSPs. Accumulation of misfolded proteins in the endoplasmic reticulum (ER) activates the unfolded protein response (UPR), leading to induction of transcripts involved in ER-quality control (ERQC) and ER-associated degradation (ERAD) pathways, thereby alleviating ER stress. As a result of active HSR and UPR, aggregate formation is restricted (minimal). Short-term autophagy, potentially regulated by IRE1 -dependent and -independent pathways, efficiently clears residual aggregates, maintaining proteostasis and promoting survival. In contrast, unprimed seedlings undergo translational repression and fail to efficiently activate HSR and UPR, resulting in prolonged ER stress and excessive protein aggregation. In response, autophagy remains persistently activated but soon becomes potentially

963 maladaptive, coupled with a proteostasis collapse and ultimately leading to seedling death. *Some elements*
964 *of the illustration were taken from BioRender.com.*

965 Supplementary Figures

966 **Figure S1: Unprimed seedlings display total protein loss and sustained presence of misfolded**
967 **proteins following heat stress.** (A) SDS-PAGE analysis indicates that unprimed seedlings undergo a
968 reduction in total protein content by the end of 3 DPS, compared to primed and control (n=3 biological
969 replicates). (B-C) The *bZIP60* spliced form (*bZIP60s*) was used as a marker to detect misfolded protein
970 accumulation. RT-PCR of *bZIP60s*, *bZIP60u* and *ACT2* for all the conditions at given time points post
971 heat stress suggested that primed seedlings initially accumulate misfolded proteins but recovered by 1
972 DPS to control levels (denoted by dotted line). However, unprimed seedlings experienced sustained
973 accumulation of misfolded proteins as seen from the presence of high *bZIP60s*. Box plot represents
974 quantification for *bZIP60*(s) / *bZIP60*(s+u(unspliced)) (n=2 biological replicates). [AP - After priming;
975 BT - Before triggering; AT - After triggering (Day 0); DPS - Days post-stress].

976 **Figure S2: Transcriptome and expression analysis of primed and unprimed seedlings post heat**
977 **stress.** (A) Schematic representation of sampling time points for transcriptome analysis. Seedlings was
978 exposed to a priming stimulus (PS) followed by a triggering stimulus (TS) (primed), only a TS (unprimed),
979 or no treatment (control). Samples were collected after priming (AP), immediately after triggering (AT; 0
980 DPS), and one day post-stress (1 DPS) (n=2 biological replicates). (B) Principal component analysis
981 (PCA) of transcriptome profiles shows distinct transcriptional reprogramming induced by priming, with
982 AP_primed samples separating strongly from unprimed and control. Upon triggering and during recovery,
983 AT_primed and 1 DPS_primed shift closer to unprimed and control respectively. Unprimed (AT and 1
984 DPS) and control (AP, AT and 1 DPS) samples form a tighter cluster, indicating transcriptional similarity
985 across samples. (C) Bar plot shows differentially expressed genes (DEGs) in primed and unprimed
986 seedlings (n=2 biological replicates). A total of 6727 unique DEGs were identified with thresholds of log2
987 fold change ≥ 1 or ≤ -1 and a false discovery rate (FDR) < 0.01. The pie charts on top indicate the
988 percentage of upregulated or downregulated DEGs for each condition. (D) The heatmap represents mean
989 gene expression levels post-priming/triggering heat stress. Expression of *HSP21*, *HSP22*, *HSP70* and
990 *HSP101* reflects fold change compared to control. In the primed, *HSPs* get highly induced upon priming
991 and triggering compared to the control. In contrast, in the unprimed, induced expression for most of the
992 *HSPs* is observed in only 1 DPS. The data are presented as mean ± SD (n=3 biological replicates). (E)
993 Heatmap represents mean gene expression levels of *HSFA1a*, *HSFA2* and *HSFA3* post-priming/triggering
994 heat stress. *HSFA1a* expression (except AT/1 DPS in unprimed) did not significantly change across time
995 points, whereas *HSFA2* and *HSFA3* expression significantly increased immediately after priming (n=3
996 biological replicates). Statistical significance was calculated using one-way ANOVA (**** $p < 0.0001$;
997 *** $p < 0.001$; ** $p < 0.01$; * $p < 0.05$; ns - not significant). [DPS - Days post-stress].

998 **Figure S3: Unprimed seedlings experience translational arrest following triggering heat stress.** (A)
999 The heatmap shows the mean expression levels of differentially expressed genes associated with protein
1000 translation, including ribosomal proteins and RNA polymerases, derived from the transcriptome data. The

1001 priming stimulus alone (AP) does not alter the expression of these genes. However, upon triggering stress
1002 (AT), both primed and unprimed seedlings exhibited a marked downregulation, indicative of translational
1003 repression. During the recovery phase (1 DPS), primed seedlings restore the expression of translation-
1004 associated genes to near-control levels, whereas unprimed seedlings displayed reduced expression,
1005 suggesting a sustained translational arrest. (B) Immunoblot analysis showing induced levels of HSP101
1006 in primed (both soluble and insoluble fractions) post-stress compared to control. HSP101 was undetectable
1007 in both the fractions of the unprimed seedlings, indicating an arrest of protein translation following heat
1008 stress (n=2 biological replicates). [AP - After priming; AT - After triggering (Day 0); DPS - Days post-
1009 stress, C - Control, P - Primed, UP - Unprimed].

1010 **Figure S4: Loss of bZIP60 or IRE1A/B leads to delayed heat shock response.** (A) Quantification of
1011 immunoblots revealed that HSP17.6 displays a similar pattern of increase in protein levels post-priming,
1012 across genotypes, compared to WT. A delay in the maximal induction of other HSPs was observed in the
1013 mutants compared to WT (n=3 biological replicates). (B) Heatmap represents the mean gene expression
1014 levels of *HSP21*, *HSP22*, *HSP70* and *HSP101* in *bzip60* and *ire1a/b* lines post-priming/triggering heat
1015 stress. In the primed, *HSPs* were highly induced upon priming and triggering, whereas, in the unprimed,
1016 induced expression of most of the *HSPs* was observed only by 1 DPS (n=2/3 biological replicates).
1017 Statistical significance was calculated using one-way ANOVA (**** $p < 0.0001$; *** $p < 0.001$; ** p
1018 < 0.01; * $p < 0.05$; ns - not significant) [AP - After priming, BT - Before triggering, AT - After triggering
1019 (Day 0), DPS - Days post-stress].

1020 **Figure S5: Priming-mediated autophagy response is TOR/SnRK independent**. Immunoblot analysis
1021 of pS6K, S6K, and pAMPK under all the conditions at the given time points. (A-B) TOR kinase activity,
1022 as measured by pS6K/S6K levels, remained similar post-priming and triggering across conditions
1023 compared to control during priming/heat stress. The numbers below denote represents normalised mean
1024 intensity of pS6K/S6K respect to corresponding control time point (n=2 biological replicates). (C-D) The
1025 pAMPK/α-Tub levels do not change post-priming and triggering across conditions compared to control,
1026 indicating that SnRK activity remains similar during priming/heat stress. The numbers below denote
1027 represents normalised mean intensity of pAMPK/α-Tub respect to corresponding control time point (n=2
1028 biological replicates). α-Tubulin served as a loading control. [AP- After Priming, DPS - Days Post Stress,
1029 C - Control, P - Primed, UP - Unprimed].

1030 **Figure S6: Autophagy remained induced in *bzip60* and *ire1a/b* mutants post-heat stress.** Western blot
1031 analysis of ATG8 in (A) *bzip60* and (B) *ire1a/b* mutants post-heat stress revealed that autophagy was
1032 induced post-triggering (0 DPS) in primed seedlings; however, it reverted back to control levels during
1033 the stress recovery period (1-3 DPS). However, in unprimed (*bzip60* and *ire1a/b*), autophagy was induced
1034 post-triggering stress and stayed high even after removal of stress (n=3 biological replicates). α-Tubulin
1035 served as a loading control.

1036 **Figure S7: Transcript abundance of selective autophagy receptors in primed and unprimed.** Relative
1037 transcript abundance of known selective autophagy receptors, *NBR1* (next-to-BRCA1) and ATG8-
1038 interacting protein 1 (*ATI1*), 2 (*ATI2*) and 3 (*ATI3*), was obtained from transcriptome data collected post-

heat stress. All four genes were upregulated following priming stimulus (AP), whereas unprimed seedlings do not show change in expression. The preferential induction of these receptors suggests that selective autophagy may be activated in the primed seedlings following heat stress. [AP - After priming, AT - After triggering (Day 0), DPS - Days post-stress].

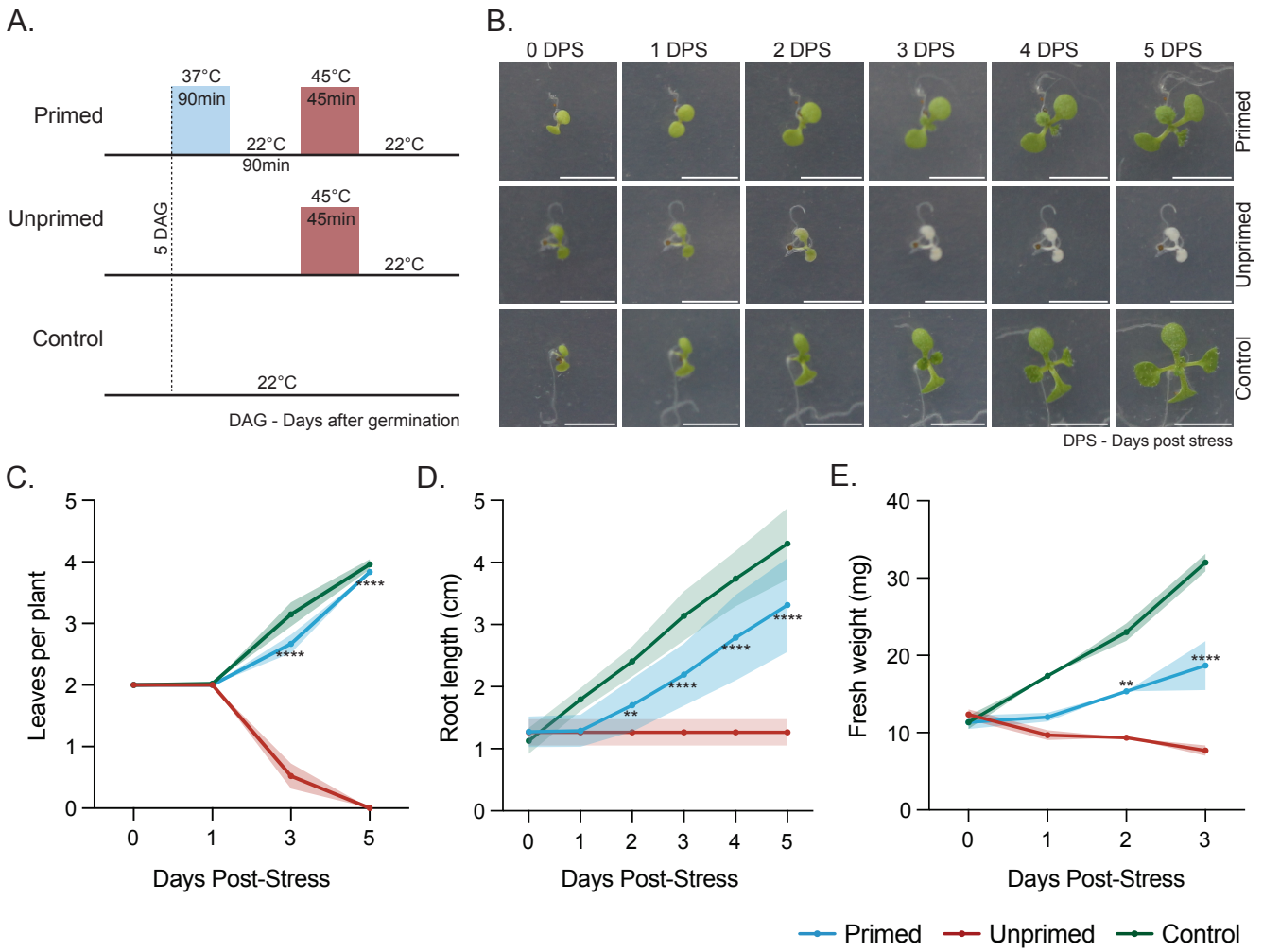

Figure 1: Priming improves survival under severe heat stress. (A) The experimental paradigm is schematised where 37°C was used as a priming stimulus, followed by recovery at 22°C (optimal growth temperature), and then exposed to a 45°C heat-triggering stimulus for the indicated time durations. Control (untreated) and unprimed seedlings (subjected to only 45°C) were compared in parallel. (B) Post-heat stress, seedlings were monitored over multiple days at 22°C to assess their recovery. The panel depicts representative images for primed, unprimed and control conditions. Scale bar, 0.5cm. The growth recovery was quantified based on (C) the number of leaves per plant (n=3 biological replicates, with 16 seedlings per replicate), (D) root length (n=3 biological replicates, with 6 seedlings per replicate), and (E) fresh weight (n=3 biological replicates, with 16 seedlings pooled per replicate) at the indicated time points. Despite an initial halt in growth (as observed in root length), primed seedlings resumed growth similar to the control, whereas unprimed plants exhibited complete growth arrest and ultimately failed to survive. Data are presented as mean ± SEM (for leaves per plant) and mean ± SD (for root length and fresh weight). Statistical significance was determined using two-way ANOVA, where the asterisk (** $p < 0.01$; **** $p < 0.0001$) indicates significant differences between the primed and unprimed seedlings.

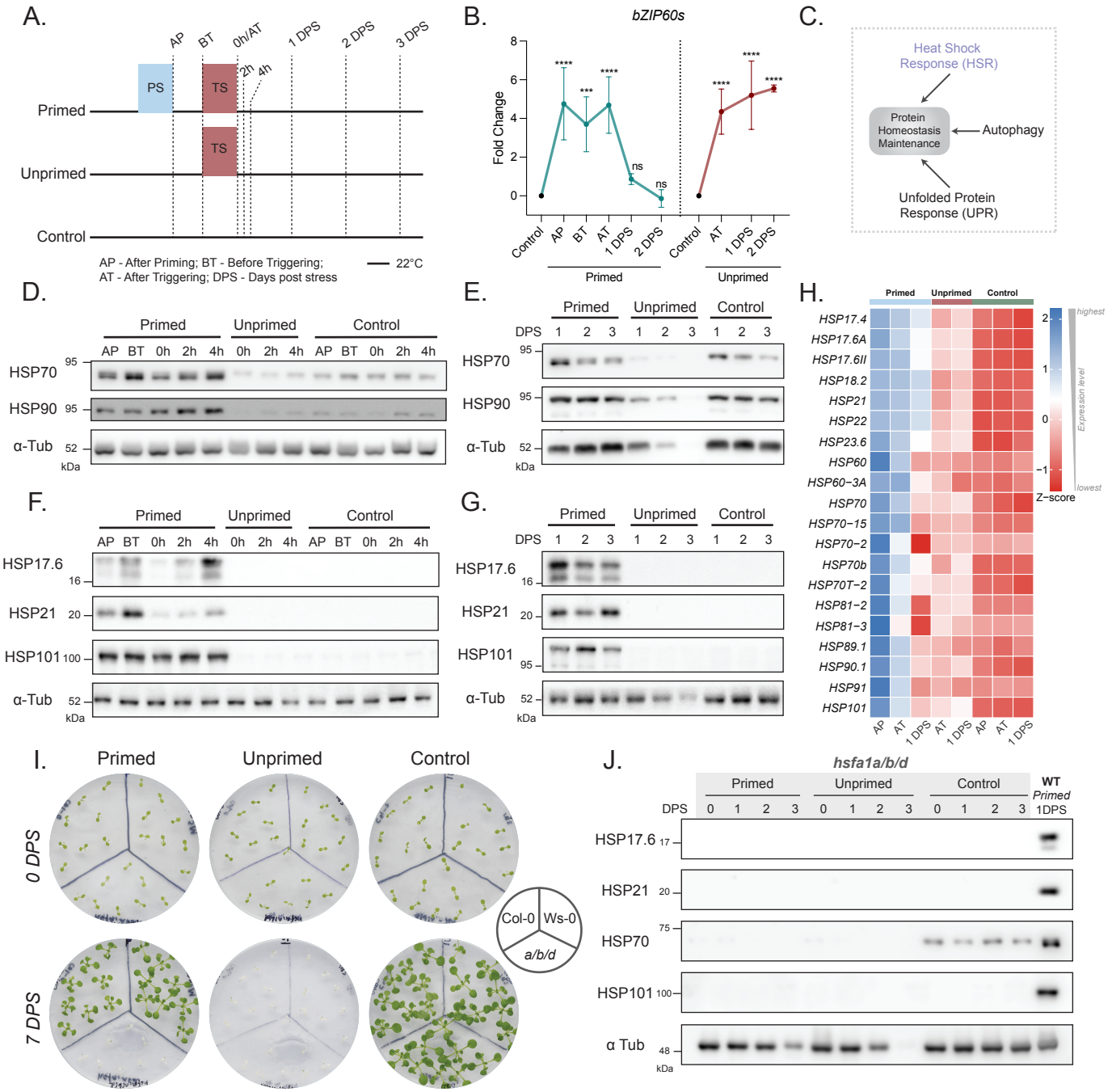

Figure 2: Priming leads to an increase in chaperone abundance post-heat stress via HSFA1. (A) The schematics of the experimental paradigm is shown. AP, BT, and 0-3 DPS denote the time points at which seedlings were collected (PS-Priming Stimulus, TS-Triggering Stimulus). (B) Misfolded protein accumulation following heat stress was determined by checking for the presence of *bZIP60* spliced form (*bZIP60s*). Expression analysis suggested that primed seedlings initially accumulated misfolded proteins but recovered by 1 DPS, whereas unprimed seedlings experienced a sustained accumulation of misfolded proteins (n=3 biological replicates). Statistical significance was calculated using one-way ANOVA (**** p <0.0001; *** p <0.001; ns – not significant). (C) Illustrated representation of the processes involved in the maintenance of protein homeostasis. (D-G) To assess the status of HSR, western blot analysis of HSP17.6, HSP21, HSP70, HSP90, and HSP101 proteins in various samples was performed post-heat stress. The data revealed that priming led to an increase in the abundance of HSPs, which persisted even after stress removal. In contrast, unprimed seedlings did not show any increase in HSP abundance compared with the control (n=3 biological replicates). α-Tubulin served as a loading control. (H) Heat map showing the mean expression levels of *HSPs* across different time points, derived from transcriptome data (n=2 biological replicates). The data suggests that priming stimulus led to an increase in *HSP* levels compared to control. Unprimed seedlings also displayed an increase in *HSP* abundance post-stress compared to control, but the level remained lower than that of primed seedlings. (I) The panel depicts representative images of *hsfa1a/b/d* (referred to as *a/b/d*), Col-0 and Ws-0 post-priming/triggering heat stress. The effect of priming on heat stress response was lost in the *a/b/d* mutant compared to Col-0/Ws-0. Unprimed *a/b/d* failed to survive, similar to that of Col-0/Ws-0 post-heat stress (n=3 biological replicates). (J) Immunoblot analysis of HSPs revealed that primed-WT displayed an increased abundance post-priming, whereas primed *a/b/d* failed to display HSP abundance (n=3 biological replicates).

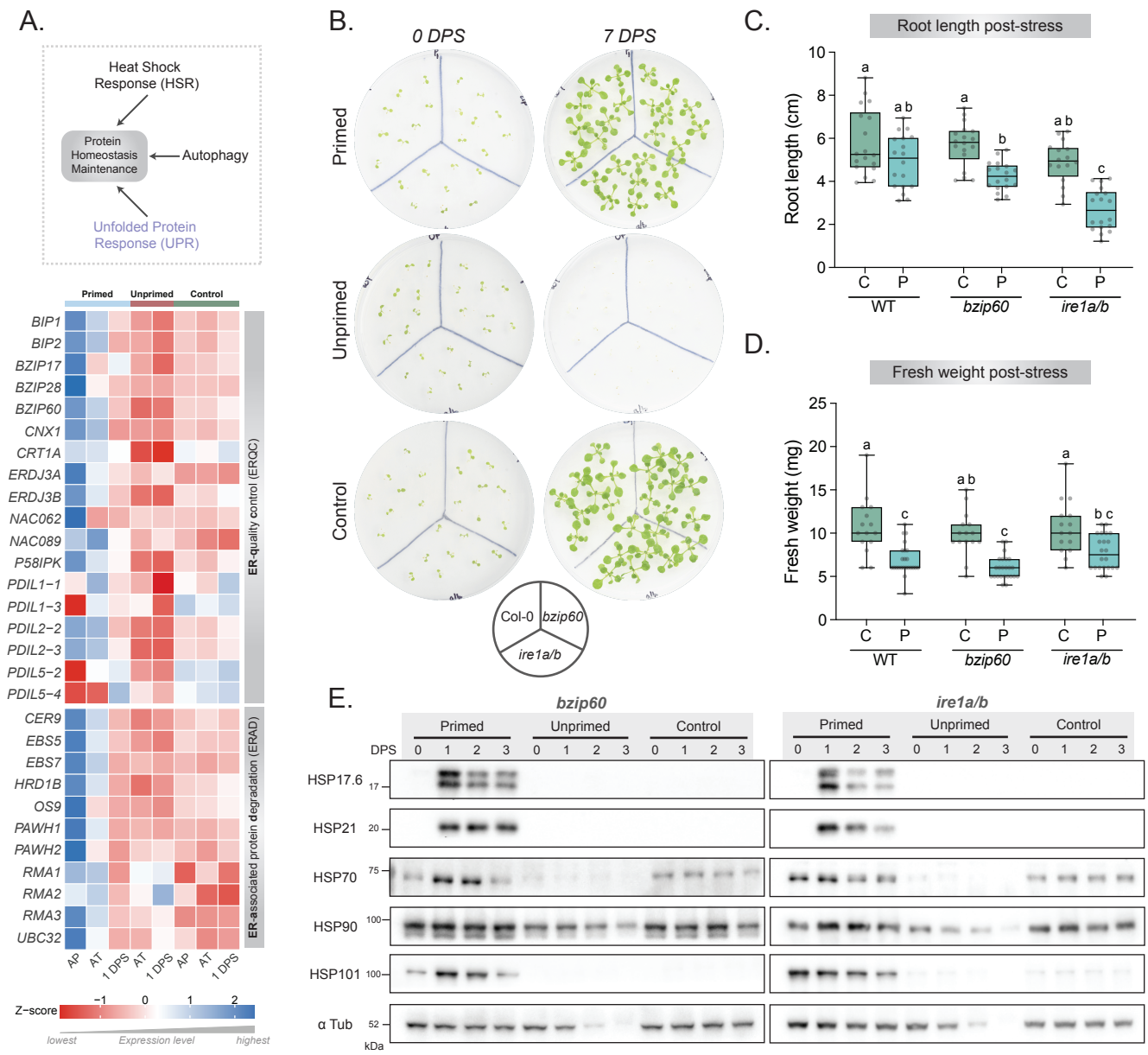

Figure 3: Priming stimulus activates the transcriptional unfolded protein response, while loss of UPR delays seedling recovery post-heat stress. (A) Transcriptome data was used to assess unfolded protein response (UPR) following heat stress. The heatmap displays the mean expression levels of genes involved in endoplasmic reticulum (ER) quality control (ERQC) and ER-associated degradation (ERAD), representing two major branches of the UPR pathway. Primed seedlings exhibited enhanced activation of UPR genes compared to control, whereas unprimed seedlings fail to induce a comparable response following heat stress. (B) Panel depicts representative images of UPR mutants, *bzip60* and *ire1a/b* lines, post-priming/triggering heat stress. Primed *bzip60* and *ire1a/b* knockout mutants survived severe heat stress, whereas the unprimed seedlings failed to survive (n=3 biological replicates). (C-D) Primary root length and fresh weight were quantified at 7 DPS across all genotypes. For WT, primed seedlings showed comparable root length to control, whereas, primed *bzip60* and *ire1a/b* mutants showed a significant reduction in root length compared to their respective controls. Fresh weight was found to be reduced in primed seedlings of all genotypes when compared to their respective control. On the x-axis, C denotes control and P denotes primed seedlings. Data are presented as median ± SD (n=3 biological replicates, comprising a total of 15-24 seedlings represented as individual grey circles). Statistical significance was assessed using one-way ANOVA followed by Tukey's post-hoc test. Compact letter display was used to denote statistically significant differences among groups ($p < 0.05$); groups not sharing a common letter are significantly different. (E) To assess the HSR status in *bzip60* and *ire1a/b* mutants, western blot analysis of HSP17.6, HSP21, HSP70, HSP90, and HSP101 proteins was performed for all the conditions post-heat stress. The data revealed that priming led to an increase in the abundance of HSPs in *bzip60* and *ire1a/b*, which persisted even after the stress removal, indicating an active HSR in the mutants. Unprimed *bzip60* and *ire1a/b* seedlings did not show any increase in HSP levels, similar to unprimed wild-type (n=3 biological replicates). [AP - After priming; AT - After triggering (Day 0); DPS - Days post-stress].

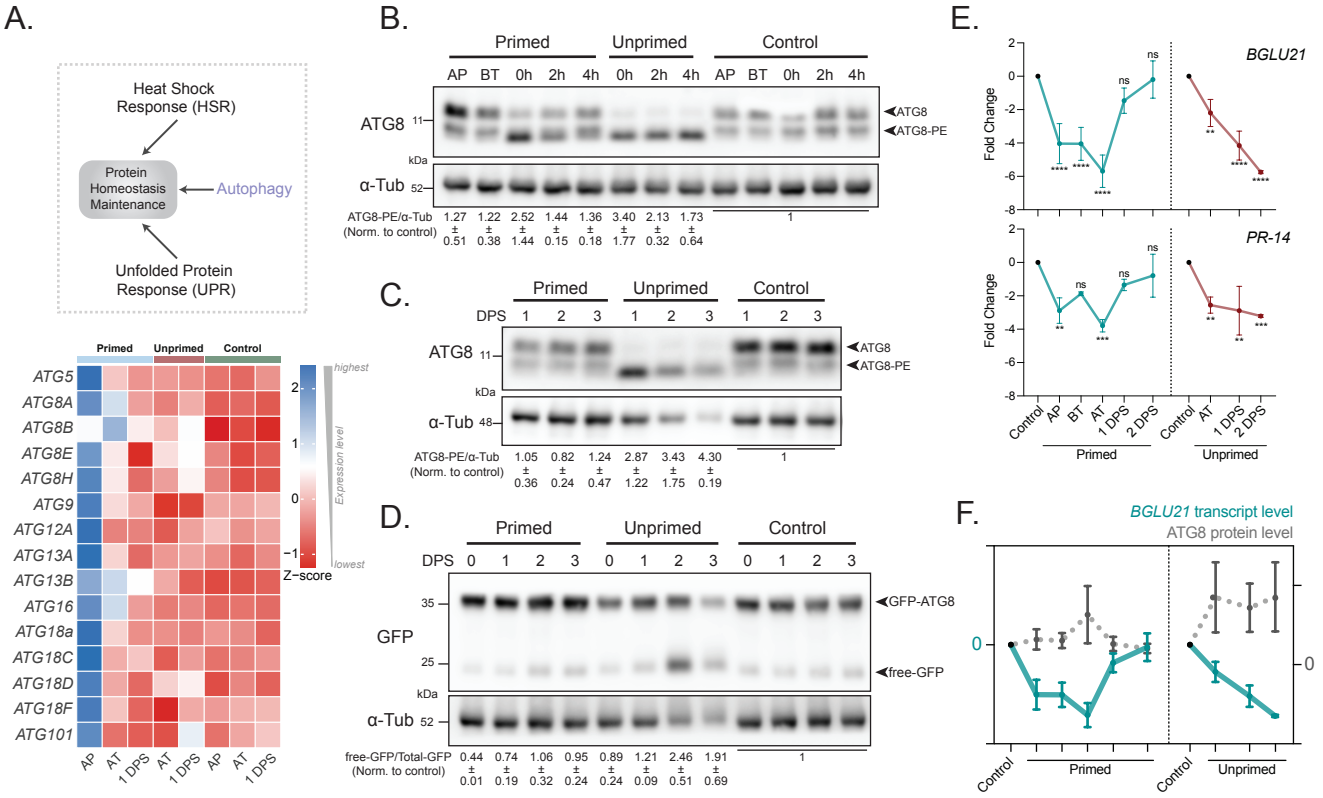

Figure 4: Primed seedlings display temporary autophagy, whereas unprimed seedlings experience sustained autophagy. (A) The heat map shows the mean expression levels of differentially expressed autophagy-related genes (ATGs) across time points, derived from transcriptome analysis. The data indicate that the priming stimulus leads to an increase in the expression of ATGs compared to the control. (B-C) Western blot analysis of ATG8 revealed that primed seedlings showed slightly induced autophagy (as seen by ATG8-PE levels) compared to control at the AP time point, which increased further post-triggering stress (0h to 4h). However, at 1 DPS, autophagy in primed is comparable to control levels. In contrast, unprimed seedlings displayed a surge in the ATG8-PE levels post-stress (0h) that remained continuously higher compared to the control. Numbers below denote intensity values post-normalisation with respect to the corresponding control time point (n=3 biological replicates). (D) Western blot of GFP-ATG8 and free-GFP (both detected using anti-GFP antibody) for various samples at the post-heat stress time points revealed that autophagy flux in unprimed seedlings remained high during the stress recovery period, as seen by the high free-GFP levels, whereas autophagy in primed seedlings was similar to that of the control. Numbers below represent normalised mean intensity of free-GFP/Total-GFP (GFP-ATG8+free-GFP) with respect to the corresponding control time point (n=2 biological replicates). (E) Expression of autophagy inhibitors *BGLU21* and *PR-14* is represented as fold change compared to control. In primed, expression of autophagy inhibitors was found to be downregulated at AP, BT and AT timepoints, but it returned to control levels by 1 DPS. However, in unprimed, autophagy inhibitors were continuously maintained at lower levels post-stress. The data are presented as mean ± SD (n=2/3 biological replicates). Statistical significance was calculated using one-way ANOVA (**** $p < 0.0001$; *** $p < 0.001$; ** $p < 0.01$; ns - not significant). (F) Data-driven illustrated representation depicting the correlation between the downregulation of the autophagy inhibitor *BGLU21* coinciding with the induction of ATG8 levels in primed and unprimed seedlings. [AP - After priming; BT - Before triggering; AT - After triggering (Day 0); DPS - Days post-stress].

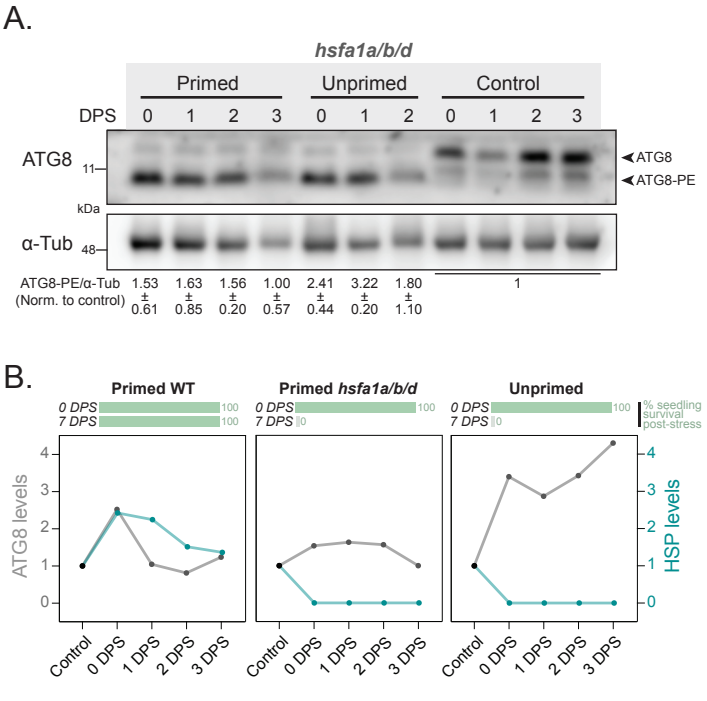

Figure 5: Impairment of the heat shock response amplifies autophagy during proteotoxic stress. (A) Western blot analysis of ATG8 in *hsfa1a/b/d* mutants shows that autophagy remains highly induced in both primed and unprimed following heat stress (n=3 biological replicates). The numbers below denote intensity values post-normalisation with respect to corresponding control timepoint. (B) Data-driven illustrated line plots comparing ATG8 and HSP abundance profiles in primed WT, primed *hsfa1a/b/d*, and unprimed seedlings at the indicated timepoints. The bar plots above indicate the percentage of seedling survival at 7 DPS (n=3 biological replicates per condition). In primed WT, chaperone accumulation (HSPs) peaks early and is accompanied by transient ATG8 induction, suggesting efficient proteostasis and resolution of stress via timely attenuation of autophagy. Conversely, both unprimed WT and primed *hsfa1a/b/d* mutants failed to induce HSPs, correlating with sustained ATG8 accumulation and complete post-stress mortality. Collectively, these data illustrate that thermotolerance is driven by a coordinated HSP-autophagy interplay, whereas its failure leads to autophagy overactivation and seedling lethality. [DPS - Days post stress].

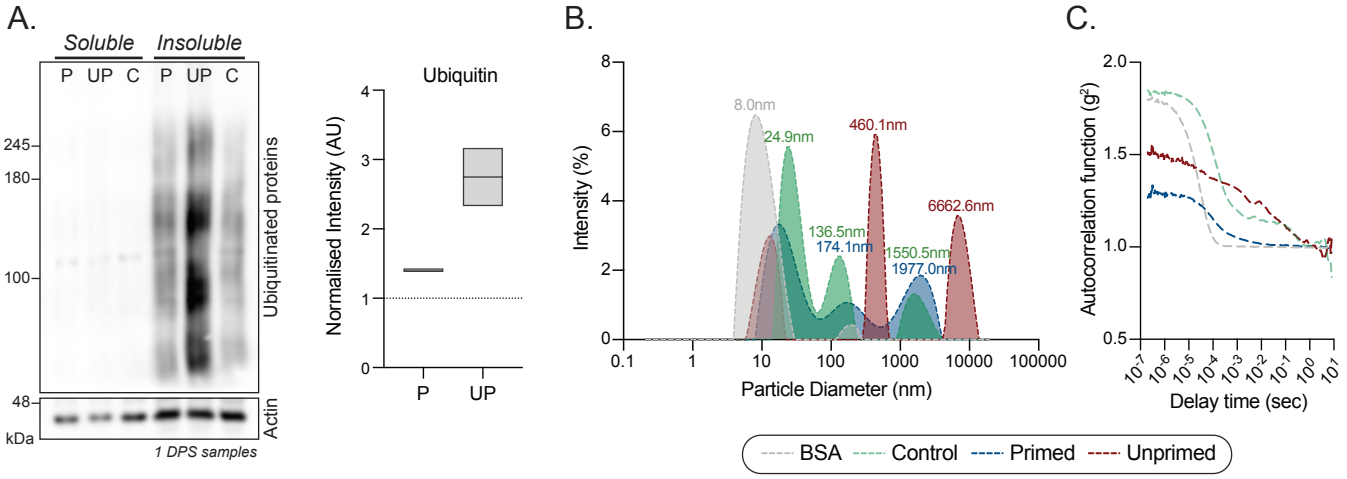

Figure 6: Priming facilitates effective aggregate clearance following heat stress. (A) Immunoblot analysis of ubiquitin-conjugated aggregates shows that unprimed seedlings have a higher accumulation of aggregates compared to primed and control seedlings by 1 DPS. Box plot represents the normalised mean intensity for ubiquitin in the insoluble fraction. The dotted line denotes the control value (n=2 biological replicates). (B) Dynamic Light Scattering (DLS) analysis showing the particle size distribution of protein aggregates isolated at 1 DPS from control, primed, and unprimed seedlings. Bovine serum albumin (BSA) was used as a monomeric protein standard. Unprimed seedlings accumulated a higher proportion of large aggregates (460.1 nm and 6662.6 nm), indicating extensive aggregation. In contrast, primed seedlings displayed smaller aggregate populations (174.1 nm and 1977.0 nm), comparable to control, suggesting more efficient aggregate clearance. (C) Autocorrelation function (g^2) curves derived from DLS measurements reflect particle size dynamics and diffusion behavior. BSA exhibited the steepest/fastest decay, consistent with uniform small particles. Aggregates derived from unprimed seedlings exhibited the slowest decay, reflective of larger, less diffusive aggregate populations. Primed samples show a faster decay than unprimed, indicating smaller and more dynamic aggregates. Data is representative of two biological replicates.

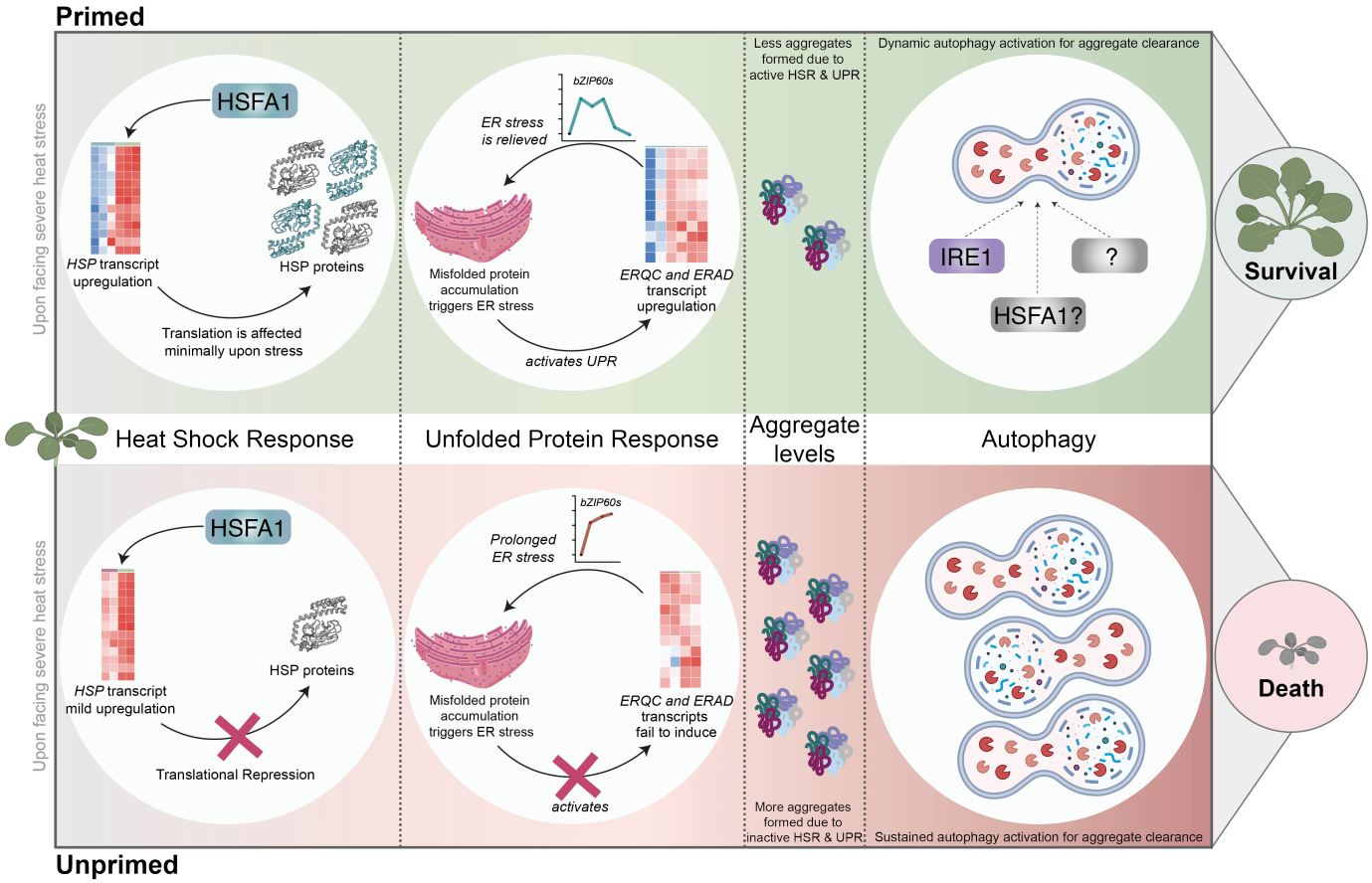

Figure 7: Priming-mediated acquired thermotolerance underlies dynamic regulation of proteostasis. The illustration compares the responses of primed (top panel) and unprimed (bottom panel) Arabidopsis seedlings upon exposure to severe heat stress. In primed seedlings, HSFA1-mediated transcriptional activation drives a robust heat shock response (HSR) associated with accumulation of HSPs. Accumulation of misfolded proteins in the endoplasmic reticulum (ER) activates the unfolded protein response (UPR), leading to induction of transcripts involved in ER-quality control (ERQC) and ER-associated degradation (ERAD) pathways, thereby alleviating ER stress. As a result of active HSR and UPR, aggregate formation is restricted (minimal). Short-term autophagy, potentially regulated by IRE1 -dependent and -independent pathways, efficiently clears residual aggregates, maintaining proteostasis and promoting survival. In contrast, unprimed seedlings undergo translational repression and fail to efficiently activate HSR and UPR, resulting in prolonged ER stress and excessive protein aggregation. In response, autophagy remains persistently activated but soon becomes potentially maladaptive, coupled with a proteostasis collapse and ultimately leading to seedling death. *Some elements of the illustration were taken from BioRender.com*.

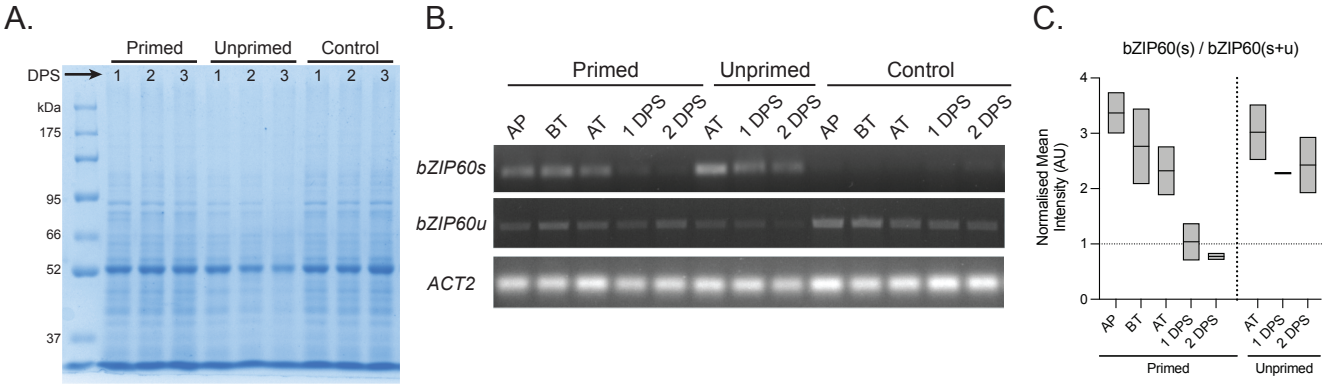

Figure S1: Unprimed seedlings display total protein loss and sustained presence of misfolded proteins following heat stress. (A) SDS-PAGE analysis indicates that unprimed seedlings undergo a reduction in total protein content by the end of 3 DPS, compared to primed and control (n=3 biological replicates). (B-C) The *bZIP60* spliced form (*bZIP60s*) was used as a marker to detect misfolded protein accumulation. RT-PCR of *bZIP60s*, *bZIP60u* and *ACT2* for all the conditions at given time points post heat stress suggested that primed seedlings initially accumulate misfolded proteins but recovered by 1 DPS to control levels (denoted by dotted line). However, unprimed seedlings experienced sustained accumulation of misfolded proteins as seen from the presence of high *bZIP60s*. Box plot represents quantification for *bZIP60*(s) / *bZIP60*(s+u(unspliced)) (n=2 biological replicates). [AP - After priming; BT - Before triggering; AT - After triggering (Day 0); DPS - Days post-stress].

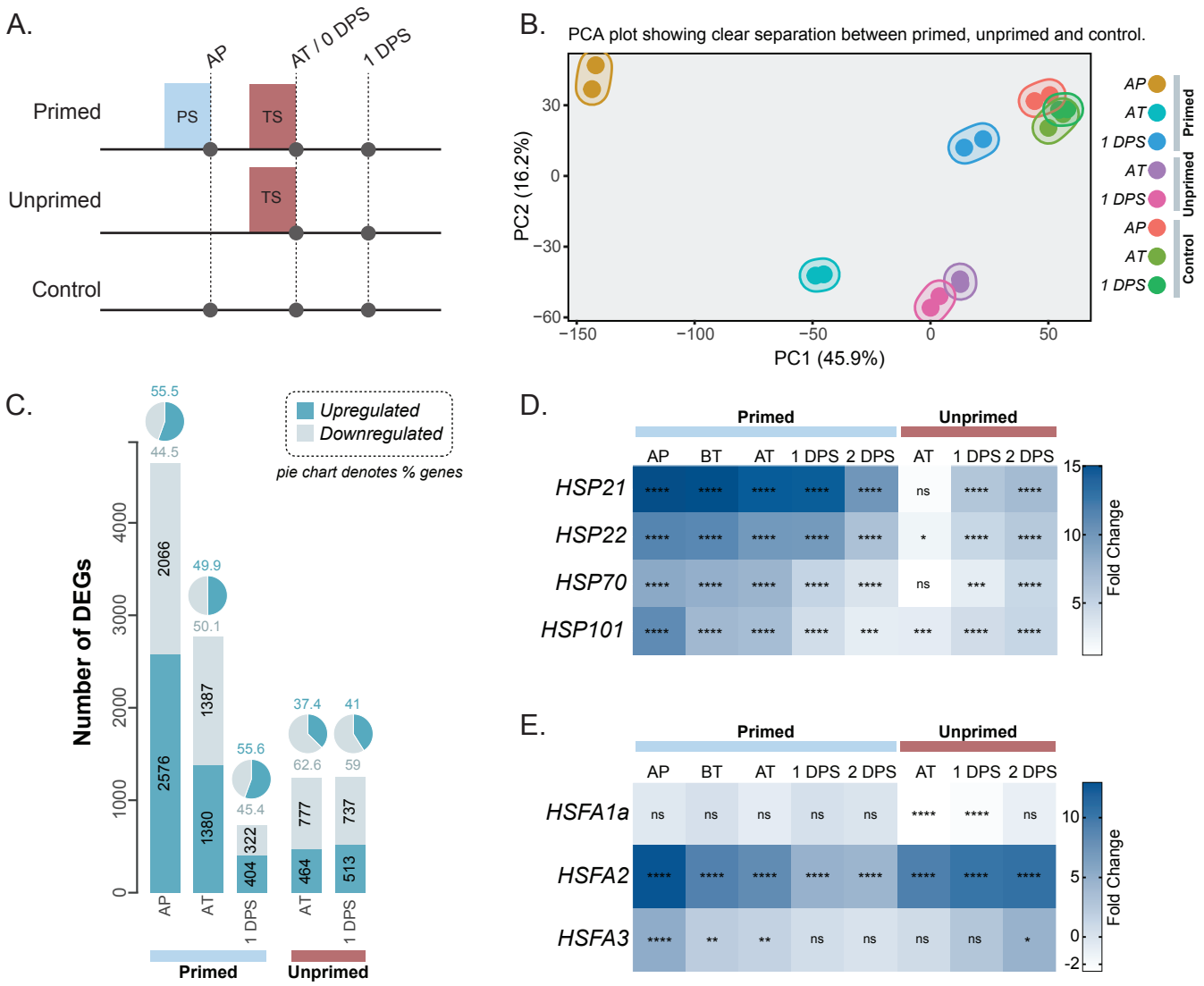

Figure S2: Transcriptome and expression analysis of primed and unprimed seedlings post heat stress. (A) Schematic representation of sampling time points for transcriptome analysis. Seedlings was exposed to a priming stimulus (PS) followed by a triggering stimulus (TS) (primed), only a TS (unprimed), or no treatment (control). Samples were collected after priming (AP), immediately after triggering (AT; 0 DPS), and one day post-stress (1 DPS) (n=2 biological replicates). (B) Principal component analysis (PCA) of transcriptome profiles shows distinct transcriptional reprogramming induced by priming, with AP_primed samples separating strongly from unprimed and control. Upon triggering and during recovery, AT_primed and 1 DPS_primed shift closer to unprimed and control respectively. Unprimed (AT and 1 DPS) and control (AP, AT and 1 DPS) samples form a tighter cluster, indicating transcriptional similarity across samples. (C) Bar plot shows differentially expressed genes (DEGs) in primed and unprimed seedlings (n=2 biological replicates). A total of 6727 unique DEGs were identified with thresholds of log2 fold change ≥ 1 or ≤ –1 and a false discovery rate (FDR) < 0.01. The pie charts on top indicate the percentage of upregulated or downregulated DEGs for each condition. (D) The heatmap represents mean gene expression levels post-priming/triggering heat stress. Expression of *HSP21, HSP22, HSP70* and *HSP101* reflects fold change compared to control. In the primed, *HSPs* get highly induced upon priming and triggering compared to the control. In contrast, in the unprimed, induced expression for most of the *HSPs* is observed in only 1 DPS. The data are presented as mean ± SD (n=3 biological replicates). (E) Heatmap represents mean gene expression levels of *HSFA1a, HSFA2* and *HSFA3* post-priming/triggering heat stress. *HSFA1a* expression (except AT/1 DPS in unprimed) did not significantly change across time points, whereas *HSFA2* and *HSFA3* expression significantly increased immediately after priming (n=3 biological replicates). Statistical significance was calculated using one-way ANOVA (**** p <0.0001; *** p <0.001; ** p <0.01; * p <0.05; ns - not significant). [DPS - Days post-stress].

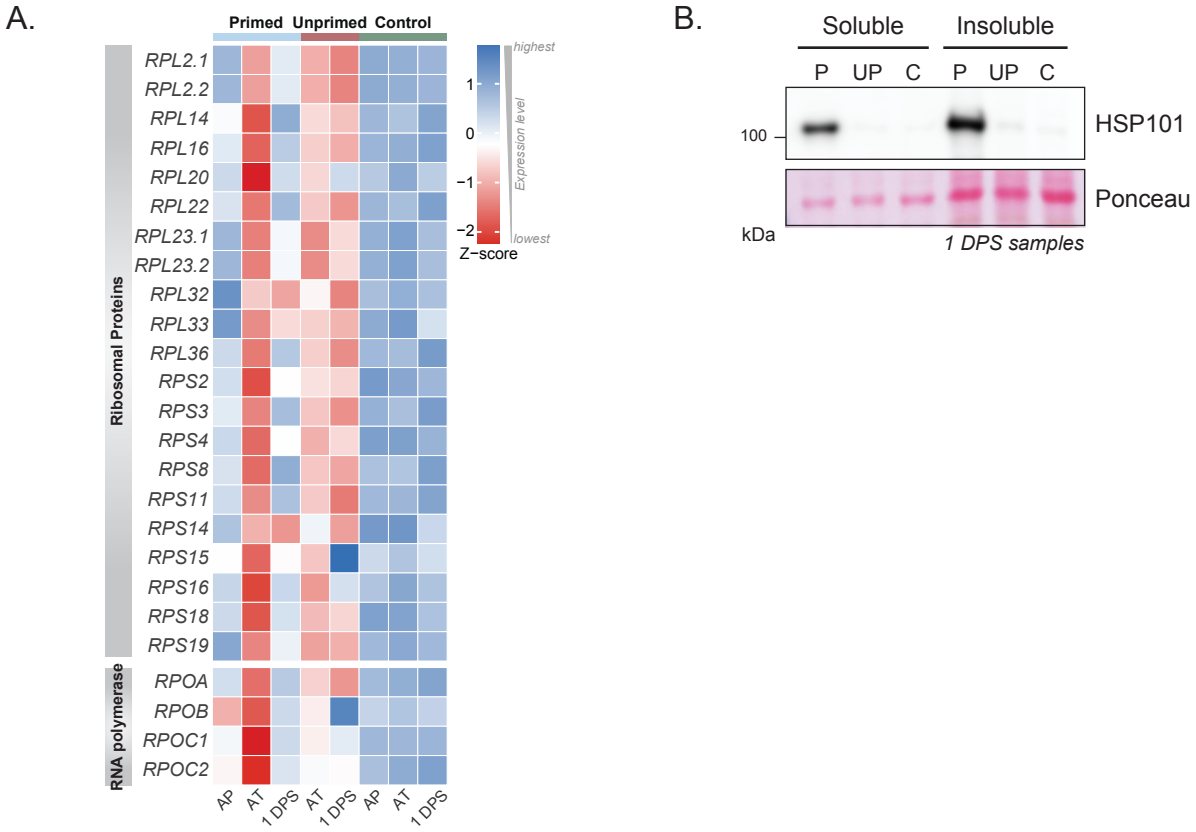

Figure S3: Unprimed seedlings experience translational arrest following triggering heat stress. (A) The heatmap shows the mean expression levels of differentially expressed genes associated with protein translation, including ribosomal proteins and RNA polymerases, derived from the transcriptome data. The priming stimulus alone (AP) does not alter the expression of these genes. However, upon triggering stress (AT), both primed and unprimed seedlings exhibited a marked downregulation, indicative of translational repression. During the recovery phase (1 DPS), primed seedlings restore the expression of translation-associated genes to near-control levels, whereas unprimed seedlings displayed reduced expression, suggesting a sustained translational arrest. (B) Immunoblot analysis showing induced levels of HSP101 in primed (both soluble and insoluble fractions) post-stress compared to control. HSP101 was undetectable in both the fractions of the unprimed seedlings, indicating an arrest of protein translation following heat stress (n=2 biological replicates). [AP - After priming; AT - After triggering (Day 0); DPS - Days post-stress, C - Control, P - Primed, UP - Unprimed].

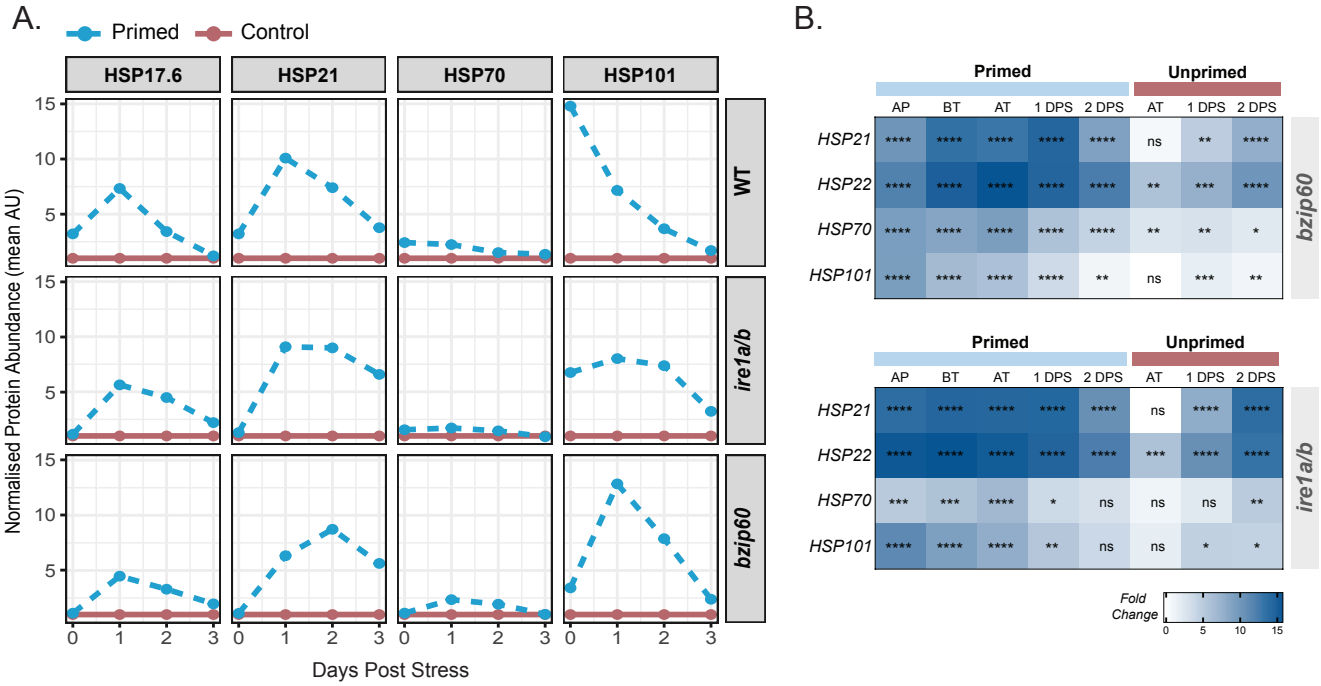

Figure S4: Loss of bZIP60 or IRE1A/B leads to delayed heat shock response. (A) Quantification of immunoblots revealed that HSP17.6 displays a similar pattern of increase in protein levels post-priming, across genotypes, compared to WT. A delay in the maximal induction of other HSPs was observed in the mutants compared to WT (n=3 biological replicates). (B) Heatmap represents the mean gene expression levels of *HSP21, HSP22, HSP70* and *HSP101* in *bzip60* and *ire1a/b* lines post-priming/triggering heat stress. In the primed, *HSPs* were highly induced upon priming and triggering, whereas, in the unprimed, induced expression of most of the *HSPs* was observed only by 1 DPS (n=2/3 biological replicates). Statistical significance was calculated using one-way ANOVA (**** p <0.0001; *** p <0.001; ** p <0.01; * p <0.05; ns – not significant) [AP - After priming, BT - Before triggering, AT - After triggering (Day 0), DPS - Days post-stress].

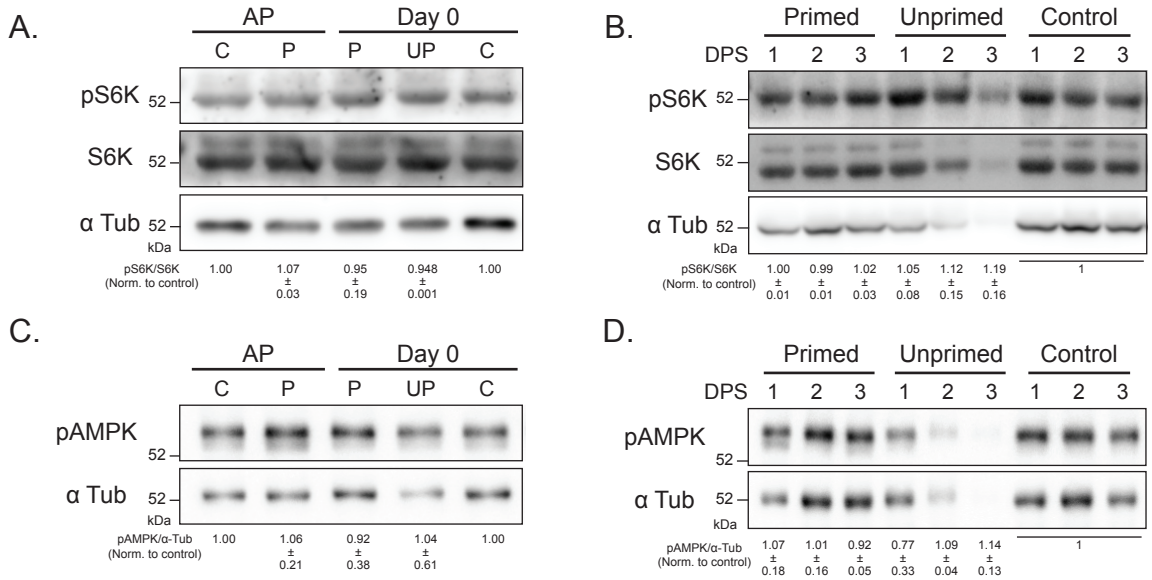

Figure S5: Priming-mediated autophagy response is TOR/SnRK independent. Immunoblot analysis of pS6K, S6K, and pAMPK under all the conditions at the given time points. (A-B) TOR kinase activity, as measured by pS6K/S6K levels, remained similar post-priming and triggering across conditions compared to control during priming/heat stress. The numbers below denote represents normalised mean intensity of pS6K/S6K respect to corresponding control time point (n=2 biological replicates). (C-D) The pAMPK/α-Tub levels do not change post-priming and triggering across conditions compared to control, indicating that SnRK activity remains similar during priming/heat stress. The numbers below denote represents normalised mean intensity of pAMPK/α-Tub respect to corresponding control time point (n=2 biological replicates). α-Tubulin served as a loading control. [AP- After Priming, DPS - Days Post Stress, C - Control, P - Primed, UP - Unprimed].

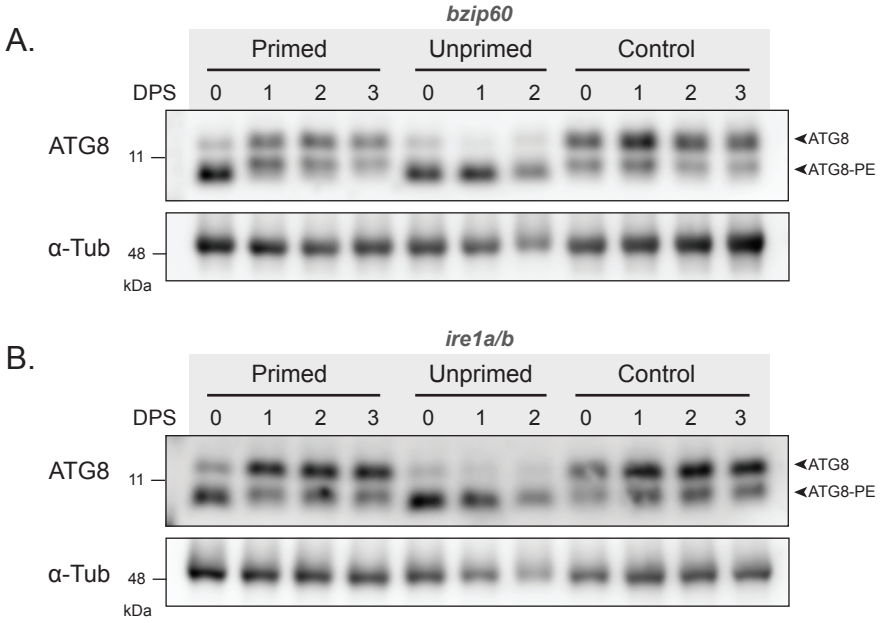

Figure S6: Autophagy remained induced in *bzip60* and *ire1a/b* mutants post-heat stress. Western blot analysis of ATG8 in (A) *bzip60* and (B) *ire1a/b* mutants post-heat stress revealed that autophagy was induced post-triggering (0 DPS) in primed seedlings; however, it reverted back to control levels during the stress recovery period (1-3 DPS). However, in unprimed (*bzip60* and *ire1a/b*), autophagy was induced post-triggering stress and stayed high even after removal of stress (n=3 biological replicates). α-Tubulin served as a loading control.

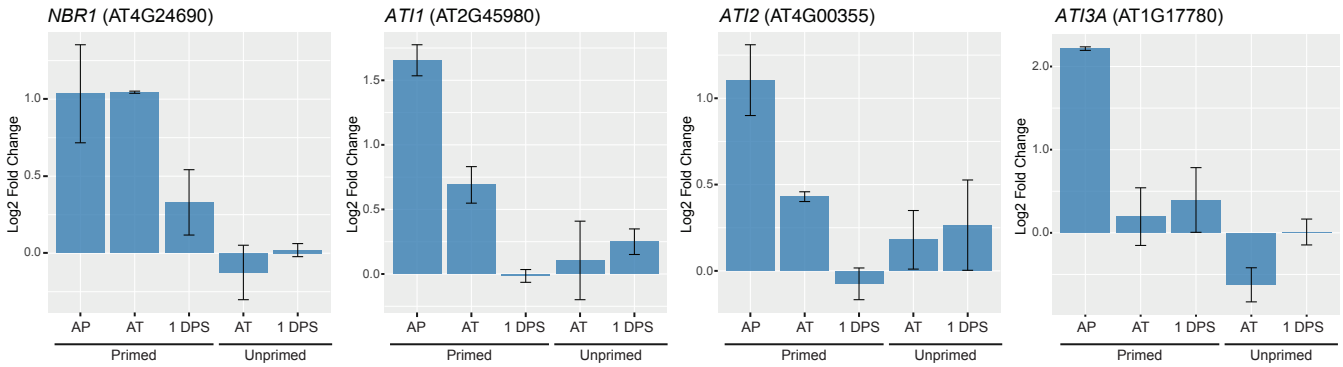

Figure S7: Transcript abundance of selective autophagy receptors in primed and unprimed. Relative transcript abundance of known selective autophagy receptors, *NBR1* (next-to-BRCA1) and ATG8-interacting protein 1 (*ATI1*), 2 (*ATI2*) and 3 (*ATI3*), was obtained from transcriptome data collected post-heat stress. All four genes were upregulated following priming stimulus (AP), whereas unprimed seedlings do not show change in expression. The preferential induction of these receptors suggests that selective autophagy may be activated in the primed seedlings following heat stress. [AP - After priming, AT - After triggering (Day 0), DPS - Days post-stress].

Gene	Accession ID	Forward Primer	Reverse Primer
ACT2	AT3G18780.2	TCTTCCGCTCTTTCTTTCCAAGC	ACCATTGTCACACACGATTGGTTG
HSP21	AT4G27670.1	AGGGAACCAAGGATCAAGTGTCG	GGTGACAAAGGATCCAACAATCCG
HSP22	AT4G10250.1	AGACCGGTTCCCTGATCCATTC	TGTGTCCCTCTCGAGTCCTAATG
HSP70	AT3G12580.1	CTACCAACACCGTCTTCGATGC	GACTCTTATCCGCTTGAACAGAGG
HSP101	AT1G74310.1	CTCTTGCTGAGCAGCTGTTTGATG	ACCTTCCTCGTGACCAACATACCC
bZIP60*	AT1G42990.1	ATGGCGGAGGAATTTGGAAGC	TCACGCCGCAAGGGTTAAGAT
bZIP60s*	-	GAAGGAGACGATGATGCTGTGGCT	AGCAGGGAACCCAACAGCAGACT
BGLU21	AT1G66270.1	TGAGAAGCCAGATCCGTCTAAACC	GGCGCTGTGATCTACATTCTTAGG
PR-14	AT5G01870.1	AGTGCGGTGTCAAACTTCCTTAC	CTCACTTAATGCTGTTGCAGTTGG
HSFA1a	AT4G17750.1	TCTTGACGGGTTCTCATCTCCAA	CAATCTCGGGGTCTTCGGGT
HSFA2	AT2G26150.1	GGTTTCGACGGGGAGGTTGA	CGCCTCATCATCGATTGCTGC
HSFA3	AT5G03720.1	AGGAGGGGAGGTGGTGAAGT	TCCCAGCAGACATCAGGCAAA

* - referred from Bao, Y., Pu, Y., Yu, X., Gregory, B. D., Srivastava, R., Howell, S. H., & Bassham, D. C. (2018). IRE1B degrades RNAs encoding proteins that interfere with the induction of autophagy by ER stress in Arabidopsis thaliana. *Autophagy*, *14*(9), 1562–1573. https://doi.org/10.1080/15548627.2018.1462426/SUPPL_FILE/KAUP_A_1462426_SM0835.DOCX

Supplementary Table 1: List of gene accession IDs and PCR primers